# BIOLOGICAL PHYSICS

*Energy, Information, Life*

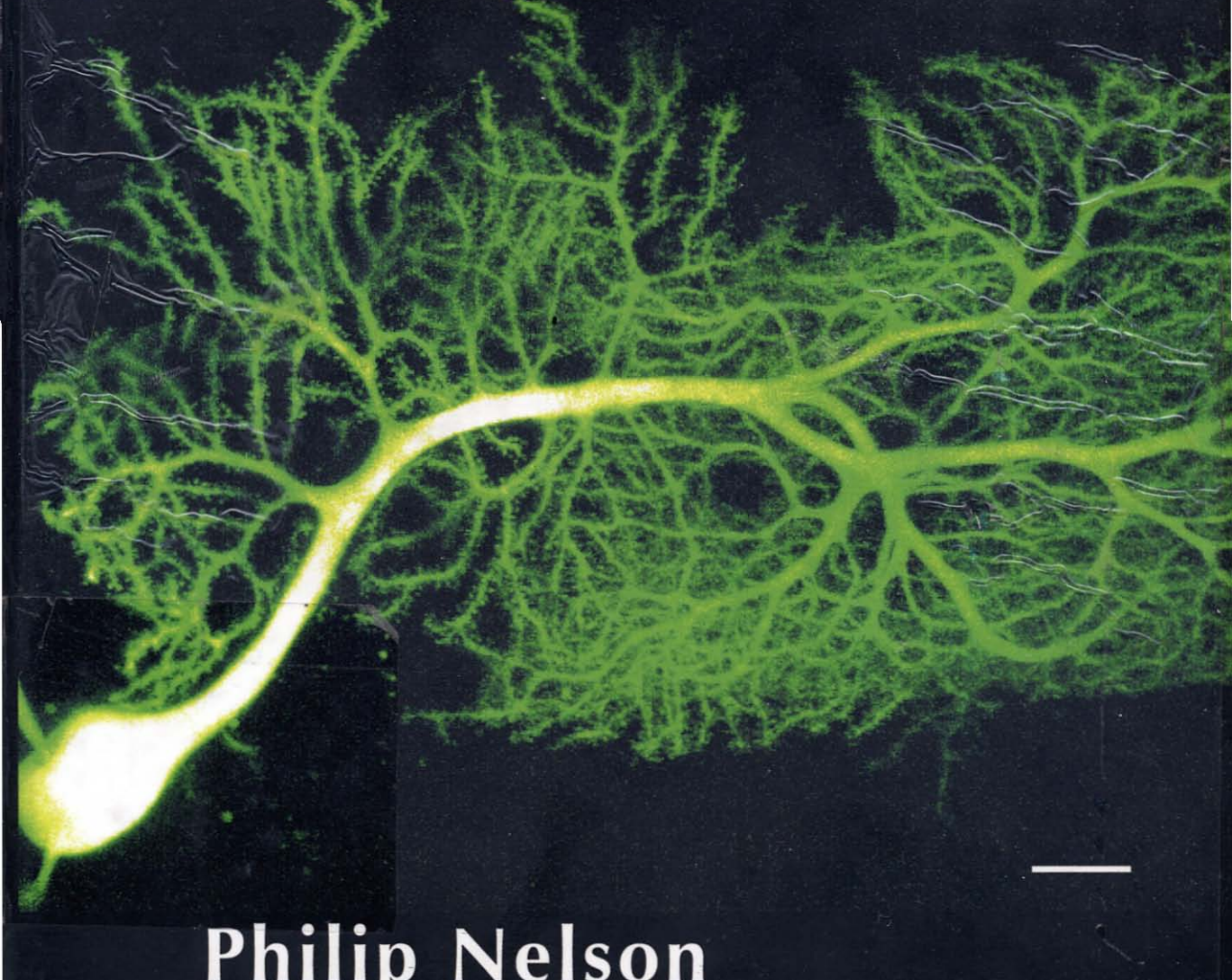

**Philip Nelson**

# Chapter 10

# Enzymes and molecular machines

If ever to a theory I should say:
'You are so beautiful!' and 'Stay! Oh, stay!'
Then you may chain me up and say goodbye—
Then I'll be glad to crawl away and die.
– Delbrück and von Weizacker's update to *Faust*, 1932

A constantly recurring theme of this book has been the idea that living organisms transduce free energy. For example, Chapter 1 discussed how animals eat high-energy molecules and excrete lower-energy molecules, generating not only thermal energy but also mechanical work. We have constructed a framework of ideas allegedly useful for understanding free energy transduction, and even presented some primitive examples of how it can work:

- Chapter 1 introduced the osmotic machine (Section 1.2.2); Chapter 7 worked through the details (Section 7.2).
- Section 6.5.3 introduced a motor driven by temperature differences.

Neither of the devices mentioned above is a very good analog of the sort of motors we find in living organisms, however, since neither is driven by chemical forces. Chapter 8 set the stage for the analysis of more biologically relevant machines, developing the notion that chemical bond energy is just another form of free energy. For example, the change $\Delta G$ of chemical potential in a chemical reaction was interpreted as a force driving that reaction: The sign of $\Delta G$ determines in which direction a reaction will proceed. But we stopped short of explaining how a molecular machine can *harness* a chemical force to drive an otherwise unfavorable transaction, such as doing mechanical work on a load. Understanding how molecules can act as free energy brokers, sitting at the interface between the mechanical and chemical worlds, will be a major goal of this chapter.

Interest in molecular machines blossomed with the realization that much of cellular behavior and architecture depends on the active, directed transport of macromolecules, membranes, or chromosomes within the cell's cytoplasm. Just as disruption of traffic hurts the functioning of a city, so defective molecular transport can result in a variety of diseases.

The subject of molecular machines is vast. Rather than survey the field, this chapter will focus on showing how we can take some familiar mechanical ideas from the macroworld, add just one new

©2000 Philip C. Nelson

ingredient (thermal motion), and obtain a rough picture of how molecular machines work. Thus, many important biochemical details will be omitted; just as in Chapter 9, mechanical images will serve as metaphors for subtle chemical details.

This chapter has a different character from earlier ones because some of the stories are still unfolding. After outlining some general principles in Sections 10.2–10.3, Section 10.4 will look specifically at a remarkable family of real machines, the kinesins. A kinesin molecule's head region is just $4 \times 4 \times 8\,\mathsf{nm}$ in size (smaller than the smallest transistor in your computer), and is built from just 345 amino acid residues. Indeed kinesin's head region is one of the smallest known natural molecular motors, and possibly the simplest. We will illustrate the interplay between models and experiments by examining two key experiments in some detail. Although the final picture of force generation in kinesin is still not known, still we will see how structural, biochemical, and physical measurements have interlocked to fill in many of the details.

The Focus Question for this chapter is:

*Biological question:* How does a molecular motor convert chemical energy, a *scalar* quantity, into directed motion, a *vector*?

*Physical idea:* Mechanochemical coupling arises from a free energy landscape with a direction set by the geometry of the motor and its track. The motor executes a biased random walk on this landscape.

## 10.1 Survey of molecular devices found in cells

### 10.1.1 Terminology

This chapter will use the term **molecular device** to include single molecules (or few-molecule assemblies) falling into two broad classes:

1. **Catalysts** enhance the rate of a chemical reaction. Catalysts created by cells are called **enzymes** (see Section 10.3.3).
2. **Machines** actively reverse the natural flow of some chemical or mechanical process by coupling it to another one. Machines can in turn be roughly divided:
   (a) **One-shot** machines exhaust some internal source of free energy. The osmotic machine in Section 1.2.2 on page 10 is a representative of this class.
   (b) **Cyclic** machines process some external source of free energy such as food molecules, absorbed sunlight, a difference in the concentration of some molecule across a membrane, or an electrostatic potential difference. The heat engine in Section 6.5.3 on page 189 is a representative of this class; it runs on a temperature difference between two external reservoirs. Because cyclic machines are of greatest interest to us, let us subdivide them still further:
      i. **Motors** transduce some form of free energy into motion, either linear or rotary. This chapter will discuss motors abstractly, then focus on a case study, kinesin.
      ii. **Pumps** transduce free energy to create concentration gradients.
      iii. **Synthases** transduce free energy to drive a chemical reaction, typically the synthesis of some product. An example is ATP synthase, to be discussed in Chapter 11.

A third class of molecular devices will be discussed in Chapters 11–12: the "gated ion channels" sense external conditions and respond by changing their permeability to specific ions.

Before embarking on the mathematics, Sections 10.1.2 through 10.1.4 describe a few representative classes of the molecular machines found in cells, in order to have some concrete examples in mind as we begin to develop a picture of how such machines work. (Section 10.5 briefly describes still other kinds of motors.)

### 10.1.2 Enzymes display saturation kinetics

Chapter 3 noted that a chemical reaction, despite having a favorable free energy change, may proceed very slowly due to a large activation energy barrier (Idea 3.27 on page 80). Chapter 8 pointed out that this circumstance gives cells a convenient way to store energy, for example in glucose or ATP, until it is needed. But what happens when it *is* needed? Quite generally, cells need to speed up the natural rates of many chemical reactions. The most efficient way to do this is with some reusable device—a catalyst.

Enzymes are biological catalysts. Most enzymes are made of protein, sometimes in the form of a complex with other small molecules ("coenzymes" or "prosthetic groups"). Other examples include ribozymes, which consist of RNA. Complex catalytic organelles such as the ribosome (Figure 2.33) are complexes of protein with RNA.

To get a sense of the catalytic power of enzymes, consider the decomposition of hydrogen peroxide at room temperature, $H_2O_2 \rightarrow H_2O + \frac{1}{2}O_2$. This reaction is highly favorable energetically, with $\Delta G^0 = -41 k_B T_r$, yet it proceeds very slowly in pure solution: With an initial concentration $1\,\mathrm{M}$ of hydrogen peroxide, the rate of spontaneous conversion at $25°\mathrm{C}$ is just $10^{-8}\,\mathrm{M\,s^{-1}}$. This rate corresponds to a decomposition of just 1% of a sample after two weeks. Various substances can catalyze the decomposition, however. For example, the addition of $1\,\mathrm{mM}$ hydrogen bromide speeds the reaction by a factor of 10. But the addition of the enzyme **catalase**, at a concentration of binding sites again equal to $1\,\mathrm{mM}$, results in a speedup factor of 1 000 000 000 000!

**Your Turn 10a**

Reexpress this fact by giving the number of molecules of hydrogen peroxide that a *single* catalase molecule can split per second.

In your body's cells, catalase breaks down hydrogen peroxide generated by other enzymes (as a byproduct of eliminating dangerous free radicals before they can damage the cell).

In the catalase reaction, hydrogen peroxide is called the **substrate** upon which the enzyme acts; the resulting oxygen and water are the **products**. The rate of change of the substrate concentration (here $10^4\,\mathrm{M\,s^{-1}}$) is called the **reaction velocity**. The reaction velocity clearly depends on how much enzyme is present. To get a quantity intrinsic to the enzyme itself, we divide the velocity by the concentration of enzyme[1] (taken to be $1\,\mathrm{mM}$ above). Even this number is not completely intrinsic to the enzyme, but also reflects the availability (concentration) of the substrate. But most enzymes exhibit **saturation kinetics**: The reaction velocity increases up to a point as we increase substrate concentration, then levels off. Accordingly we define the **turnover number** of an enzyme as the maximum velocity divided by the concentration of enzyme. The turnover number really is an intrinsic property: It reflects one enzyme molecule's competence at processing substrate when

[1] More precisely, we divide by the concentration of active sites, which is the concentration times the number of such sites per enzyme molecule. Thus for example catalase has four active sites; the rates quoted above actually correspond to a concentration of catalase of $0.25\,\mathrm{mM}$.

given as much substrate as it can handle. In the case of catalase, the numbers given in the previous paragraph reflect the saturated case, so the maximum turnover number is the quantity you found in Your Turn 10a.

Catalase is a speed champion among enzymes. A more typical example is fumarase, which hydrolyzes fumarate to L-malate,[2] with maximum turnover numbers somewhat above $1000\,\mathsf{s}^{-1}$. This is still an impressive figure, however: It means that a liter of $1\,\mathsf{mM}$ fumarase solution can process up to about a mole of fumarase per second, many orders of magnitude faster than a similar reaction catalyzed by an acid.

### 10.1.3 All eukaryotic cells contain cyclic motors

Section 6.5.3 made a key observation, that the efficiency of a free energy transduction process is greatest when the process involves small, controlled steps. Though we made this observation in the context of heat engines, still it should seem reasonable in the chemically driven case as well, leading us to expect that Nature should choose to build even its most powerful motors out of many subunits, each made as small as possible. Indeed, early research on muscles discovered a hierarchy of structures on shorter and shorter length scales (Figure 10.1). As each level of structure was discovered, first by optical and then by electron microscopy, each proved not to be the ultimate force generator, but rather a collection of smaller force-generating structures, right down to the molecular level. At the molecular scale, we find the origin of force residing in two proteins: **myosin** (golf-club shaped objects in Figure 10.1) and actin (spherical blobs in Figure 10.1). Actin self-assembles from its globular form (**G-actin**) into thin filaments (**F-actin**, the twisted chain of blobs in the figure), forming a track to which myosin molecules attach.

The direct proof that single actin and myosin molecules were capable of generating force came from a remarkable set of experiments, called single-molecule **motility assays**. Figure 10.2 summarizes one such experiment. A bead attached to a glass slide carries a small number of myosin molecules. A single actin filament attached at its ends to other beads is maneuvered into position over the stationary myosin using optical tweezers. The density of myosin on the bead is low enough to ensure that at most one myosin engages the filament at a time. When the fuel molecule ATP is added to the system, the actin filament is observed to take discrete steps in one definite direction away from the equilibrium position set by the optical traps; without ATP, no such stepping is seen. This directed, non-random motion occurs without any external macroscopic applied force (unlike, say, electrophoresis).

Muscles are obvious places to look for molecular motors, because they generate macroscopic forces. Other motors are needed as well, however. In conrast to muscle myosin, many other motors do not work in huge teams but rather alone, generating tiny, piconewton-scale forces. For example, Section 5.3.1 described how locomotion in *E. coli* requires a rotary motor joining the flagellum to the body of the bacterium; Figure 5.9 on page 157 shows this motor as an assembly of macromolecules just a few tens of nanometers across. In a more indirect argument, Section 4.4.1 argued that passive diffusion alone could not transport proteins and other products synthesized at one place in a cell to the distant places where they are needed; instead some sort of "trucks and highways" are needed to transport these products actively. Frequently the "trucks" consist of bilayer vesicles. The "highways" are visible in electron microscopy as long protein polymers called

[2] Fumarase plays a part in the citric acid cycle (Chapter 11), splitting a water molecule and attaching the fragments to fumarate, converting it to malate.

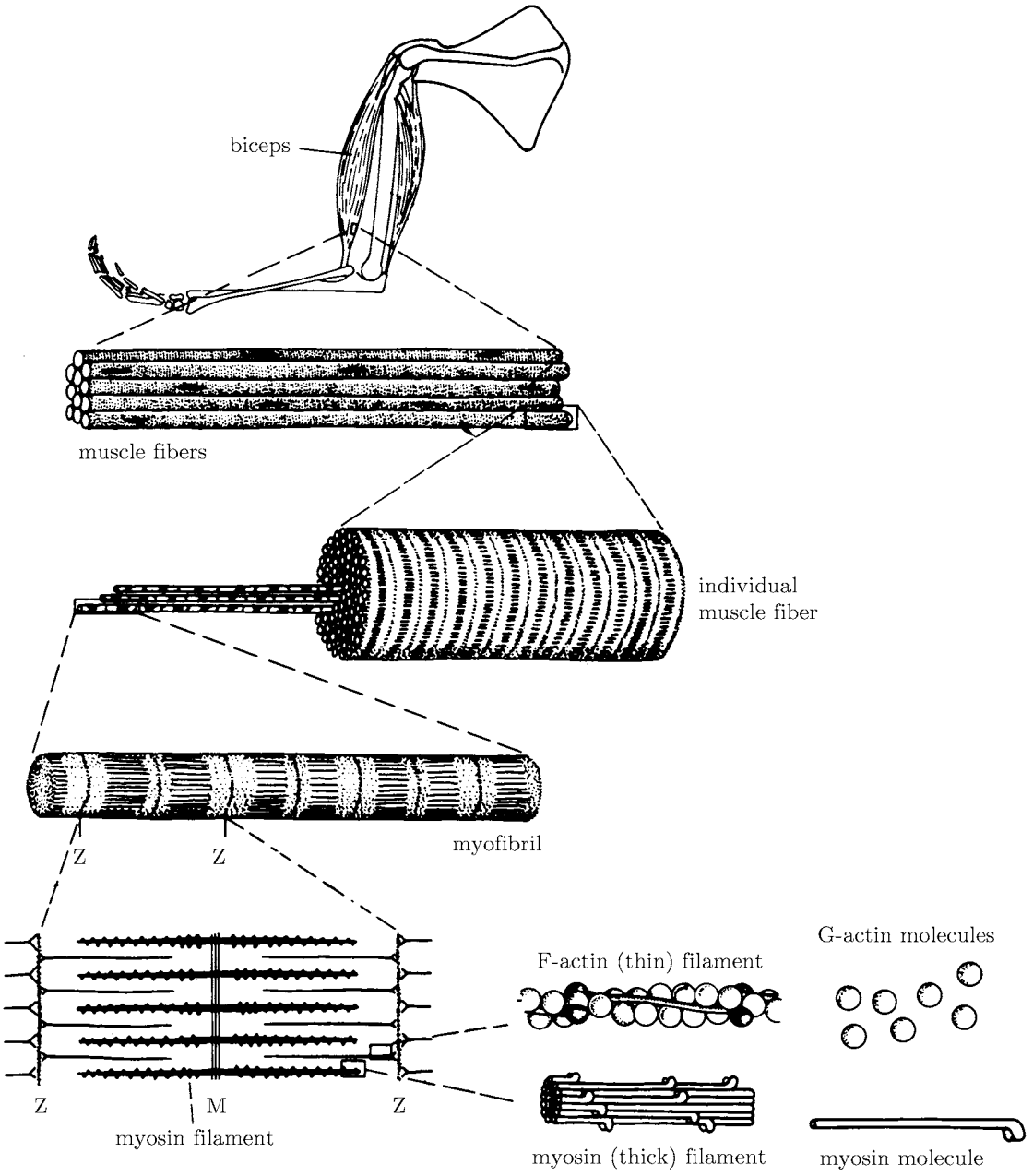


Figure 10.1: (Sketches.) Organization of skeletal muscle at successively higher magnifications. The ultimate generators of force in a myofibril (muscle cell) are bundles of myosin molecules, interleaved with actin filaments (also called "F-actin"). Upon activation, the myosins crawl along the actin fibers, pulling them toward the plane marked "M" and thus shortening the muscle fiber. [After McMahon, 1984.]

microtubules (Figure 2.26 on page 55). Somewhere between the truck and the highway there must be an "engine."

One particularly important example of such an engine, **kinesin**, was discovered in 1985, in the course of single-molecule motility assays inspired by the earlier work on myosin. Unlike the actin/myosin system, kinesin molecules are designed to walk individually along microtubules (Fig-

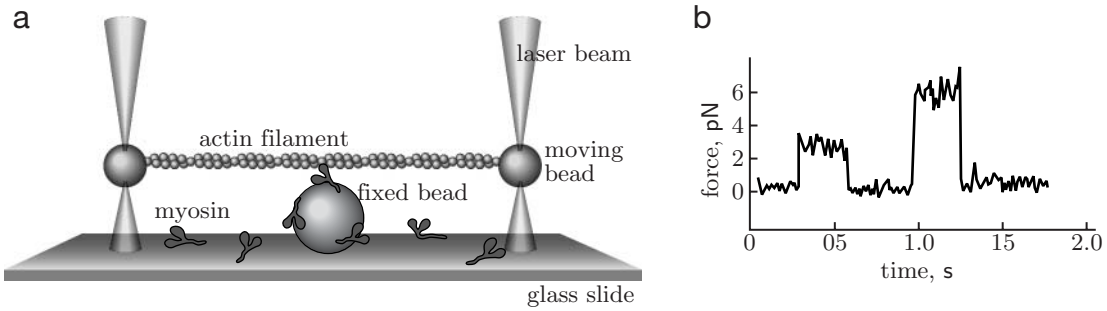


Figure 10.2: (Schematic; experimental data.) Force production by a single myosin molecule. (a) Beads are attached to the ends of an actin filament. Optical tweezers are used to manipulate the filament into position above another, fixed bead coated with myosin fragments. Forces generated by a myosin fragment pull the filament to the side, displacing the beads. The optical trap generates a known spring-like force opposing this displacement, so that the observed movement of the filament gives a measure of the force generated by the motor. (b) Force generation observed in the presence of 1 $\mu$M ATP, showing how the motor takes a step, then detaches from the filament. [After Finer et al., 1994.]

ure 2.21 on page 49): Often just one kinesin molecule carries an entire transport vesicle toward its destination. Many other organized intracellular motions, for example the separation of chromosomes during cell division, also imply the existence of motors to overcome viscous resistance to such directed motion. These motors too have been found to be in the kinesin family.[3]

For a more elaborate example of a molecular machine, recall that each cell's genetic script is arranged linearly along a long polymer, the DNA. The cell must copy (or replicate) the script (for cell division) as well as transcribe it (for protein synthesis). Your experience with cassette tapes, videotapes, and other linear storage media should make it clear that an efficient way to perform these operations is to have a single readout machine through which the script is physically pulled. The pulling of a copy requires energy, just as a motor is needed to pull the tape across the read heads of a tape player. The corresponding machines are known as DNA or RNA polymerases for the cases of replication or transcription respectively (see Section 2.3.4 on page 57). Section 5.3.5 has already noted that some of the chemical energy used by a DNA polymerase must be spent opposing rotational friction of the original DNA and the copy.

### 10.1.4 One-shot motors assist in cell locomotion and spatial organization

Myosin, kinesin, and polymerases are all examples of cyclic motors; they can take an unlimited number of steps without any change to their own structure, as long as "fuel" molecules are available in sufficient quantities. Other directed, nonrandom motions in cells do not need this property, and for them, simpler one-shot motors can suffice.

**Translocation** Some products synthesized inside cells must not only be transported some distance inside the cell, but must actually pass across a bilayer membrane to get to their destination. For example, mitochondria import certain proteins that are synthesized in the surrounding cell's

[3]We now know that both "kinesin" and "myosin" are really large families of related molecules; human cells express about 40 varieties of each. For brevity we will use these terms to denote the best-studied members in each family: muscle myosin and "conventional" kinesin.

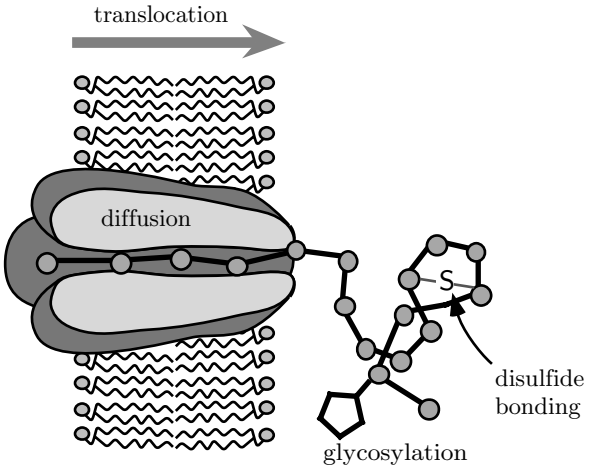


Figure 10.3: (Schematic.) Transport of a protein through a pore in a membrane. Outside the cell (right side of figure), several mechanisms can rectify the diffusive motion of the protein through the pore, for example disulfide bond formation and attachment of sugar groups (glycosylation). In addition, various chemical asymmetries between the cell's interior and exterior environment could enhance chain coiling outside the cell, preventing reentry. These asymmetries could include differences in pH and ion concentrations. [Adapted from Peskin et al., 1993.]

cytoplasm. Other proteins need to be pushed outside the cell's outer plasma membrane. Cells accomplish this "protein translocation" by threading the chain of amino acids through a membrane pore.

Figure 10.3 shows several mechanisms that can help make translocation a one-way process. This motor's "fuel" is the free energy change of the chemical modification the protein undergoes upon emerging into the extracellular environment. Once the protein is outside the cell, there is no need for further motor activity: A one-shot motor suffices for translocation.

**Polymerization** Many cells move not by cranking flagella or waving cilia (Section 5.3.1), but rather by extruding their bodies in the direction of desired motion. Such extrusions are variously called pseudopodia, filopodia, or lamellipodia (see Figure 2.11 on page 39). To overcome the viscous friction opposing such motion, the cell's interior structure (including its actin cortex; see Section 2.2.4 on page 48) must push on the cell membrane. To this end, the cell stimulates the growth of actin filaments at the leading edge. At rest, the individual (or **monomeric**) actin subunits are bound to another small molecule, profilin, which prevents them from sticking to each other. Changes in intracellular pH trigger dissociation of the actin-profilin complex when the cell needs to move; the sudden high concentration of actin monomers then avidly assemble to the ends of existing actin filaments. To confirm that actin polymerization is capable of changing a cell's shape in this way, it's possible to recreate such behavior *in vitro*. A similar experiment, involving microtubules, is shown in Figure 10.4: Here the triggered assembly of a just a handful of microtubules suffices to distend an artificial bilayer membrane.

Actin polymerization can also get coopted by parasitical organisms, including some bacteria. The most famous of these is the pathogenic bacterium *Listeria monocytogenes*, which propels itself through its host cell's cytoplasm by triggering the polymerization of the cell's own actin, forming a bundle behind it. The bundle remains stationary, enmeshed in the rest of the host cell's cytoskeleton, so the force of the polymerization motor propels the bacterium forward. Figure 10.5 shows this

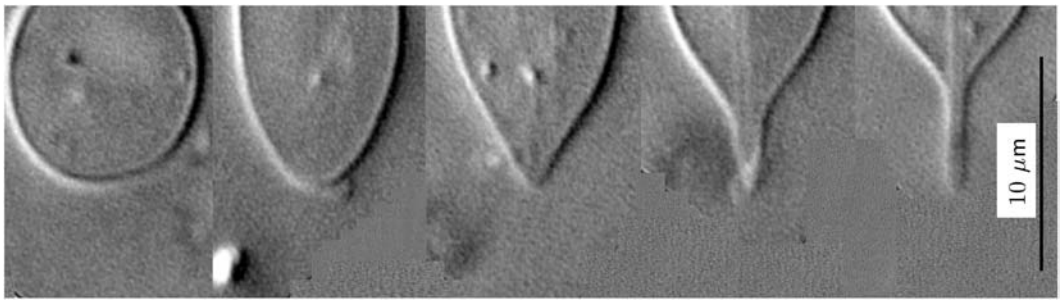


Figure 10.4: (Photomicrograph.) Microtubule polymerization distending an artificial bilayer membrane. Several microtubules gradually distort an initially spherical vesicle by growing inside it at about $2\,\mu\mathsf{m}$ per minute. [Digital image kindly supplied by D. K. Fygenson. See Fygenson et al., 1997. ]

Figure 10.5: (Photomicrograph.) Polymerization from one end of an actin bundle provides the force that propels a *Listeria* bacterium (black lozenge) through the cell surface. The long tail behind the bacterium is the network of actin filaments whose assembly it stimulated. [From Tilney & Portnoy, 1989.]

scary process at work.

Force generation by the polymerization of actin filaments or microtubules is another example of a motor, in the sense that the chemical binding energy of monomers turns into a mechanical force capable of doing useful work against the cell membrane (or invading bacterium). The motor is of the one-shot variety, because the growing filament is different (it's longer) after every step.[4]

## 10.2 Purely mechanical machines

To understand the unfamiliar we begin with the familiar. Accordingly, this section will examine some everyday macroscopic machines, show how to interpret them in the language of energy landscapes, and develop some terminology.

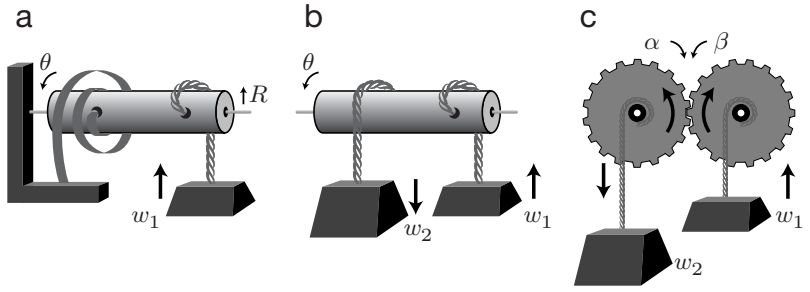


Figure 10.6: (Schematics.) Three simple macroscopic machines. In each case the weights are not considered part of the machine proper. (a) A coiled spring exerting torque $\tau$ lifts weight $w_1$, driving an increase in the angular position $\theta$. The spring is fastened to a fixed wall at one end, and to a rotating shaft at the other; the rope holding the weight winds around the shaft. (b) A weight $w_2$ falls, lifting a weight $w_1$. (c) As (b), but the shafts to which $w_1$ and $w_2$ are connected are joined by gears. The angular variables $\alpha$ and $\beta$ both decrease as $w_2$ lifts $w_1$.

### 10.2.1 Macroscopic machines can be described by an energy landscape

Figure 10.6 shows three simple, macroscopic machines. In each panel, external forces acting on the machine are symbolized by weights pulled by gravity. Panel (a) shows a simple one-shot machine: Initially, cranking a shaft of radius $R$ in the direction opposite to the arrow stores potential energy in the spiral spring. When we release the shaft, the spring unwinds, increasing the angular position $\theta$. The machine can do useful work on an external load, for example lifting a weight $w_1$, as long as $Rw_1$ is less than the torque $\tau$ exerted by the spring. If the entire apparatus is immersed in a viscous fluid, then the angular speed of rotation, $\mathrm{d}\theta/\mathrm{d}t$, will be proportional to $\tau - Rw_1$.

**Your Turn 10b**

Explain that last assertion. [*Hint:* Think back to Section 5.3.5 on page 161.]

When the spring is fully unwound, the machine stops.

Figure 10.6b shows a cyclic analog of panel (a). Here the "machine" is simply the central shaft. An external source of energy (weight $w_2$) drives an external load $w_1$ against its natural direction of motion, as long as $w_2 > w_1$. This time the machine is a broker transducing a potential energy drop in its source to a potential energy gain in its load. Once again we can imagine introducing enough viscous friction so that kinetic energy may be ignored.

Figure 10.6c introduces another level of complexity. Now we have two shafts, with angular positions $\alpha$ and $\beta$. The shafts are coupled by gears. For simplicity, suppose the gears have a 1:1 ratio, so that a full revolution of $\beta$ brings a full revolution of $\alpha$ and vice versa. As in panel (b), we may regard (c) as a cyclic machine.

Our three little machines may seem so simple that they need no further explanation. But for future use, let us pause to extract from Figure 10.6 an abstract characterization of each one.

**One-dimensional landscapes** Figure 10.7a shows a potential energy graph, or **energy landscape** , for our first machine. The lower dotted line represents the potential energy of the spring. Adding the potential energy of the load (upper dashed line) gives a total (solid line) that decreases

[4]Strictly speaking, living cells constantly recycle actin and tubulin monomers by depolymerizing filaments and microtubules and "recharging" them for future use, so perhaps we should not call this a one-shot process. Nevertheless, Figure 10.4 does show polymerization force generated in a one-shot mode.

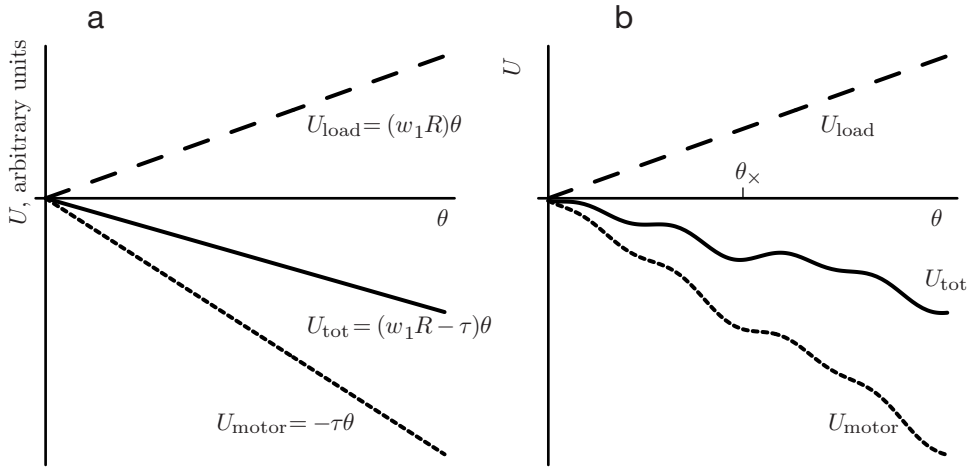


Figure 10.7: (Sketch graphs.) Energy landscapes for the one-dimensional machine in Figure 10.6a. The vertical scale is arbitrary. (a) *Lower dotted line:* The coiled spring contributes $U_{\rm motor} = -\tau\theta$ to the potential energy. *Upper dashed line:* The external load contributes $U_{\rm load} = w_1 R\theta$. *Solid line:* the total potential energy function $U_{\rm tot}(\theta)$ is the sum of these energies; it decreases in time, reflecting the frictional dissipation of mechanical energy into thermal form. (b) The same, but for an imperfect ("bumpy") shaft. *Solid curve:* Under load, the machine will stop at the point $\theta_\times$. *Lower dotted curve:* Without load, the machine will slow down, but proceed, at $\theta_\times$.

with increasing $\theta$. The slope of the total energy is downward, so $\tau = -{\rm d}U/{\rm d}\theta$ is a positive net torque. In a viscous medium the angular speed is proportional to this torque: We can think of the device as "sliding down" its energy landscape.

For the cyclic machine shown in Figure 10.6b, the graph is similar. Here $U_{\rm motor}$ is a constant, but there is a third contribution $U_{\rm drive} = -w_2 R\theta$ from the external driving weight, giving the same curve for $U_{\rm tot}(\theta)$.

Real machines are not perfect. Irregularities in the pivot may introduce bumps in the potential energy function, "sticky" spots where an extra push is needed to move forward. We can describe this effect by replacing the ideal potential energy $-\tau\theta$ by some function $U_{\rm motor}(\theta)$ (lower dotted curve in Figure 10.7b). As long as the resulting total potential energy (solid curve) is everywhere sloping downward, the machine will still run. If a bump in the potential is too large, however, then a minimum forms in $U_{\rm tot}$ (point $\theta_\times$), and the machine will stop there. Note that the meaning of "too large" depends on the load: In the example shown, the unloaded machine *can* proceed beyond $\theta_\times$. Even in the unloaded case, however, the machine will slow down at $\theta_\times$: The net torque $-{\rm d}U_{\rm tot}/{\rm d}\theta$ is small at that point, as we see by examining the slope of the dotted curve in Figure 10.7b.

To summarize, the first two machines in Figure 10.6 operate by sliding down the potential energy landscapes shown in Figure 10.7. These landscapes give "height" (that is, potential energy) in terms of one coordinate $\theta$, so we call them "one-dimensional."

**Two-dimensional landscapes** Our third machine involves gears. In the macroworld, the sort of gears we generally encounter link the angles $\alpha$ and $\beta$ together rigidly: $\alpha = \beta$, or more generally $\alpha = \beta + 2\pi n/N$, where $N$ is the number of teeth in each gear and $n$ is any integer. But we could also imagine "rubber gears," which can *slip* over each other under high load by deforming. Then the energy landscape for this machine will involve two *independent* coordinates, $\alpha$ and $\beta$. Figure 10.8 shows an imagined energy landscape for the internal energy $U_{\rm motor}$ of such gears with $N = 3$. The

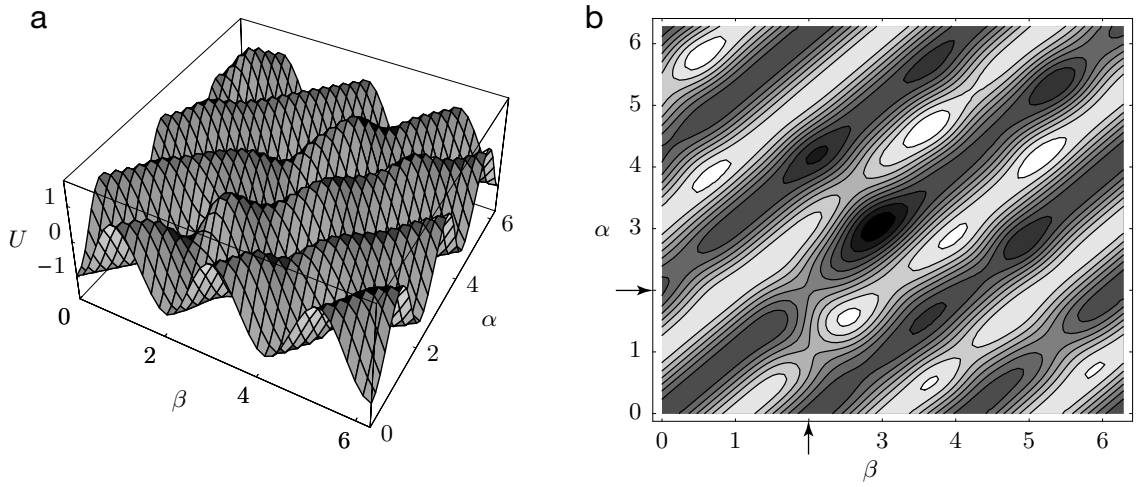


Figure 10.8: (Mathematical functions.) (a) Imagined potential energy landscape for the "bumpy rubber gears" machine in Figure 10.6c, with no load nor driving. For clarity each gear is imagined as having only three teeth. The two horizontal axes are the angles $\alpha, \beta$ in radians. The vertical axis is potential energy, with arbitrary scale. (b) The same, viewed as a contour map. The dark diagonal stripes are the valleys seen in panel (a). The valley corresponding to the main diagonal has a bump, seen as the light spot at $\beta = \alpha = 2$ (*arrows*).

preferred motions are along any of the "valleys" of this landscape, that is, the lines $\alpha = \beta + 2\pi n/3$ for any integer $n$. Imperfections in the gears have again been modeled as bumps in the energy landscape; thus the gears don't turn freely even if we stay in one of the valleys. Slipping involves hopping from one valley to the next, and is opposed by the energy ridges separating the valleys. Slipping is especially likely to occur at a bump in a valley, for example the point $(\beta = 2, \alpha = 2)$ (see the arrows in Figure 10.9b).

Now consider the effects of a load torque $w_1 R$ and a driving torque $w_2 R$ on the machine. Define the sign of $\alpha$ and $\beta$ so that $\alpha$ increases when the gear on the left turns clockwise, while $\beta$ increases when the other gear turns counterclockwise (see Figure 10.6). Thus the effect of the driving torque is to tilt the landscape downward in the direction of decreasing $\alpha$, just as in the lower dashed lines of Figure 10.7a,b. The effect of the load, however, is to tilt the landscape *upward* in the direction of decreasing $\beta$ (see Figure 10.9). The machine *slides down the landscape,* following one of the valleys. The figure shows the case where $w_1 > w_2$; here $\alpha$ and $\beta$ drive toward negative values.

Just as in the one-dimensional machine, our gears will get stuck if they attempt to cross the bump at $(\beta = 2, \alpha = 2)$, under the load and driving conditions shown. Decreasing the load could get the gears unstuck. But if we instead increased the driving force, we'd find that our machine *slips* a notch at this point, sliding from the middle valley of Figure 10.9 to the next one closer to the viewer. That is, $\alpha$ can decrease without decreasing $\beta$.

Slipping is an important new phenomenon not seen in the 1-dimensional idealization. Clearly it's bad for the machine's efficiency: A unit of driving energy gets spent ($\alpha$ decreases), but no corresponding unit of useful work is done ($\beta$ does not increase). Instead the energy all goes into

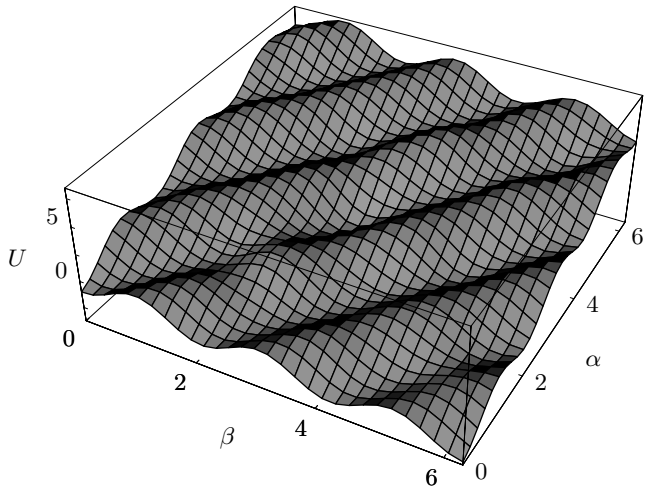


Figure 10.9: (Mathematical function.) Energy landscape for the driven, loaded, bumpy rubber gears. The landscape is the same as the one in Figure 10.8, but tilted. The figure shows the case where the driving torque is larger than the load torque; in this case the tilt favors motion to the front left of the graph. Again the scale of the vertical axis is arbitrary. The bump in the central valley (at $\beta = 2$, $\alpha = 2$) is now a spot where "slipping" is likely to occur. That is, the state of the machine can hop from one valley to the next lower one at such points.

viscous dissipation. In short:

> *The machine in Figure 10.6 stops doing useful work (that is, stops lifting the weight $w_1$) as soon as* ***either***
> *a. $w_1$ equals $w_2$, so that the machine is in mechanical equilibrium (the valleys in Figure 10.9 no longer run downhill in a direction of decreasing $\beta$), or* (10.1)
> *b. The rate of slippage becomes large.*

### 10.2.2 Microscopic machines can step past energy barriers

The machines considered in the preceding subsection were deterministic: Noise, or random fluctuations, played no important role in their operation. But we wish to study molecular machines, which occupy a nanoworld dominated by such fluctuations.

*Gilbert says:* Some surprising things can happen in this world. For example, a machine need no longer stop when it encounters a bump in the energy landscape; after a while, a large enough thermal fluctuation will always arrive to push it over the bump. In fact, I have invented a simple way to translocate a protein, using thermal motion to my advantage. I've named my device the *"G-ratchet"* in honor of myself (Figure 10.10a). It's a shaft with a series of beveled bolts; they keep the shaft from taking steps to the left. Occasionally a thermal fluctuation comes along and gives the shaft a kick with energy greater than $\epsilon$, the energy needed to compress one of the little springs holding the bolts. Then the shaft takes a step to the right.

*Sullivan:* That certainly *is* surprising. I notice that you could even use your machine to pull against a load (the external force $f$ shown in Figure 10.10).

*Gilbert:* That's right! It just slows down a bit, since now it has to wait for a thermal push with energy greater than $\epsilon + fL$ to take a step.

*Sullivan:* I have just one question: Where does the work $fL$ done against the load come from?

*Gilbert:* I guess it must come from the thermal energy giving rise to the Brownian motion....

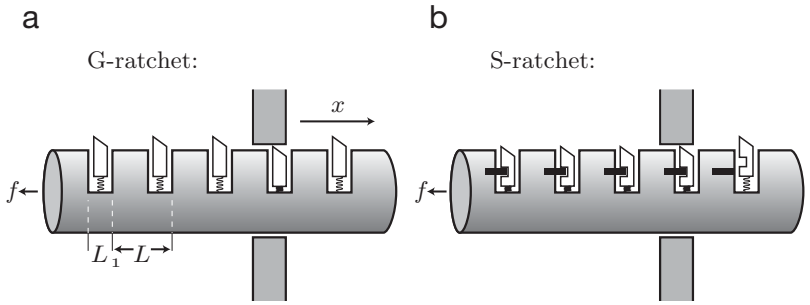


Figure 10.10: (Schematics.) (a) The "G-ratchet." A rod (horizontal cylinder) makes a supposedly one-way trip to the right through a hole in a "membrane" (shaded wall), driven by random thermal fluctuations. It's prevented from moving to the left by sliding bolts, similar to those in a door latch. The bolts can move down to allow rightward motion, then pop up as soon as they clear the wall. A possible external "load" is depicted as an applied force $f$ directed to the left. The text explains why this device does *not* work. (b) The "S-ratchet." Here the bolts are tied down on the "cell interior" (left side), then released as they emerge on the right.

*Sullivan:* Couldn't you wrap your shaft into a circle? Then your machine would go around forever, constantly doing work against a load.

*Gilbert:* Just what are you trying to tell me?

Yes, Sullivan is just about to point out that Gilbert's device would continuously extract mechanical work from the surrounding thermal motion, if it worked the way Gilbert supposes. Such a machine would spontaneously reduce the world's entropy and so violate the Second Law.[5] You can't convert thermal energy directly to mechanical energy without using up something else—think about the discussion of the osmotic motor in Section 1.2.2.

*Sullivan continues:* I think I see the flaw in your argument. It's not really so clear that your device takes only rightward steps. It cannot move at all unless the energy $\epsilon$ needed to retract a bolt is comparable to $k_{\rm B}T$. But if that's the case, then the bolts will *spontaneously* retract from time to time—they are thermally jiggling along with everything else! If a leftward thermal kick comes along at just such a moment, then the rod will take a step to the left after all.

*Gilbert:* Isn't that an extremely unlikely coincidence?

*Sullivan:* Not really. The applied force will make the rod spend most of its time pinned at one of the locations $x = 0, L, 2L, \ldots$, at which a bolt is actually touching the wall. Suppose that now a thermal fluctuation momentarily retracts the obstructing bolt. If the rod then moves slightly to the right, the applied force will just pull it right back to where it was. But if the rod moves slightly to the left, the bolt will slip under the wall and $f$ will pull the rod a full step to the left. That is, an applied force converts the random thermal motion of the rod to one-way, *left*ward, stepping. If $f = 0$, there will be no net motion at all, either to the right or left.

*Sullivan continues:* But I still like your idea. Let me propose a modification, the *"S-ratchet"* shown in Figure 10.10b. Here a latch keeps each bolt down as long as it's to the left of the wall; something releases the latch whenever a bolt moves to the right side.

*Gilbert:* I don't see how that helps at all. The bolts still never push the rod to the right.

*Sullivan:* Oh, but they do: They push on the wall whenever the rod tries to take a step to the left, and the wall pushes back. That is, they rectify its Brownian motion by bouncing off the wall.

*Gilbert:* But that's how my G-ratchet was supposed to work!

[5] Unfortunately it's already too late for Gilbert's financial backers, who didn't study thermodynamics.

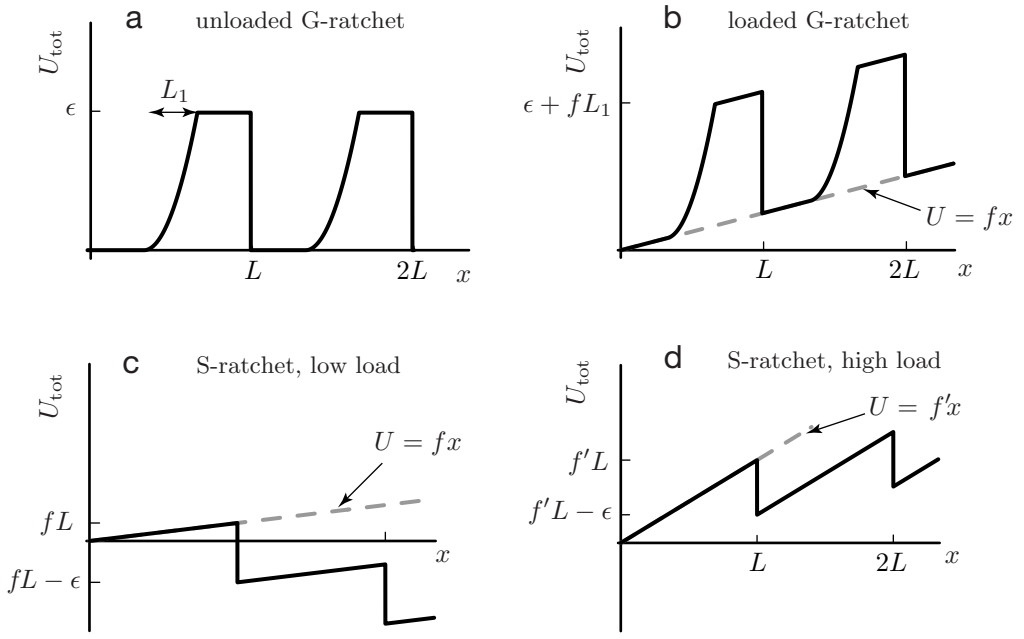


Figure 10.11: (Sketch graphs.) (a) Energy landscape of the unloaded G-ratchet (see Figure 10.10a). Pushing the rod to the right compresses the spring on one of the bolts, raising the stored potential energy by an amount $\epsilon$ and giving rise to the curved part of the graph of $U_{\rm tot}$. Once a bolt has been retracted, the potential energy is constant until it clears the wall; then the bolt pops up, releasing its spring, and the stored energy goes back down. (b) The loaded G-ratchet. Rightward motion now carries a net energy penalty, the work done against the load force $f$. Hence the graph of $U_{\rm tot}$ is tilted relative to (a). (c) The S-ratchet at low load $f$. As the rod moves rightward, its potential energy progressively decreases, as more of its bolts get released. (d) The S-ratchet at high load, $f'$. The downward steps are still of fixed height $\epsilon$, but the upward slope is greater, so that rightward progress now carries a net energy penalty.

*Sullivan:* Yes, but now something is really getting used up: The S-ratchet is a one-shot motor, releasing potential energy stored in its compressed springs as it moves. In fact, it's a mechanical analog of the translocation machine (Figure 10.3). There's no longer any obvious violation of the Second Law.

*Gilbert:* Won't your criticism of my device (that it can make backward steps) apply to yours as well?

*Sullivan:* We can design the S-ratchet's springs to be so stiff that they rarely retract spontaneously, so that leftward steps are rare. But thanks to the latches, rightward steps are still easy.

### 10.2.3 The Smoluchowski equation gives the rate of a microscopic machine

**Qualitative expectations** Let's supply our protagonists with the mathematical tools they need to clear up their controversy. Figure 10.11a,b show the energy landscapes of the G-ratchet, both without and with a load force respectively. Rightward motion of the rod compresses a spring, increasing the potential energy. At $x = 0, L, 2L, \ldots$ the bolt clears the wall. It then snaps up, dissipating the spring's potential energy into thermal form. Panels (c, d) of the figure show the energy landscape of the S-ratchet, with small and large loads ($f$ and $f'$, respectively). Again each

spring stores energy $\epsilon$ when compressed.

Note first that panel (d) is qualitatively similar to panel (b), and (a) is similar to the special case intermediate between (c,d), namely the case in which $f = \epsilon/L$. Thus we need only analyze the S-ratchet in order to find what's going on in both Gilbert's and Sullivan's devices. In brief, Sullivan has argued that

1. The unloaded G-ratchet will make no net progress in either direction, and similarly for the S-ratchet with $f = \epsilon/L$.
2. In fact, the loaded G-ratchet (or the S-ratchet with $f > \epsilon/L$) will move to the left.
3. The loaded S-ratchet, however, *will* make net progress to the right, as long as $f < \epsilon/L$.

Sullivan's remarks also imply that

4. The rate at which the loaded S-ratchet steps to the right will reflect the probability of getting a kick of energy at least $fL$, that is, enough to hop out of a local minimum of the potential shown in Figure 10.11c. The rate of stepping to the left will reflect the probability of getting a kick of energy at least $\epsilon$.

Let us begin with Sullivan's third assertion. To keep things simple, assume, as he did, that $\epsilon$ is large compared to $k_{\mathrm{B}}T$. Thus once a bolt pops up, it rarely retracts spontaneously; there is no backstepping. We'll refer to this special case of the S-ratchet as a **perfect ratchet**. Suppose at first that there's *no* external force: In our pictorial language, the energy landscape is a steep, descending staircase. Between steps the rod wanders freely with some diffusion constant $D$. A rod initially at $x = 0$ will arrive at $x = L$ in a time given approximately by $t_{\mathrm{step}} \approx L^2/2D$ (see Equation 4.5 on page 104). Once it arrives at $x = L$ another bolt pops up, preventing return, and the process repeats. Thus the average net speed is

$$\boxed{v = L/t_{\mathrm{step}} \approx 2D/L, \qquad \text{speed of unloaded, perfect S-ratchet}} \tag{10.2}$$

which is indeed positive as Sullivan claimed.

We now imagine introducing a load $f$, still keeping the perfect ratchet assumption. The key insight is now Sullivan's observation that the fraction of time a rod spends at various values of $x$ will depend on $x$, since the load force is always pushing $x$ toward one of the local minima of the energy landscape. We need to find the probability distribution, $P(x)$, to be at postion $x$.

**Mathematical framework** The motion of a single ratchet is random and complex, like any random-walker. Nevertheless, Chapter 4 showed how a simple, deterministic equation describes the *average* motion of a large collection of such walkers: The averaging eliminates details of each individual walk, leaving the simple collective behavior. Let's adapt that logic to describe a large collection of $M$ identical S-ratchets. To simplify the math further, we will also focus on just a few steps of the ratchet (say four). We can imagine that the rod has literally been bent into a circle, so that the point $x + 4L$ is the same as the point $x$. (To avoid Sullivan's criticism of the G-ratchet, we could also imagine that some external source of energy resets the bolts every time they go around.)

Initially we release all $M$ copies of our ratchet at the same point $x = x_0$, then let them walk for a long time. Eventually the ratchets' locations form a probability distribution, like the one imagined in Figure 10.12. In this distribution the individual ratchets cluster about the four potential minima

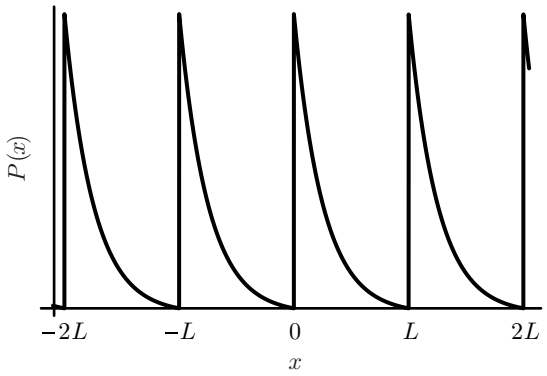


Figure 10.12: (Sketch graph.) The steady-state probability distribution for a collection of S-ratchets to be found at various positions $x$, long after all were released at a common point. We imagine the ratchet to be circular, so that $x = \pm 2L$ refer to the same point (see text). For illustration the case of a "perfect ratchet" (large energy drop, $\epsilon \gg k_B T$) has been shown; see Your Turn 10c.

(points just to the right of $x = -2L, \ldots L$), but all memory of the initial position $x_0$ has been lost. That is, $P(x)$ is a periodic function of $x$. In addition, eventually the probability distribution will stop changing in time.

The previous paragraphs should sound familiar: They amount to saying that our collection of ratchets will arrive at a quasi-steady, nonequilibrium state. We encountered such states in Section 4.6.1 on page 121, when studying diffusion through a thin tube joining two tanks with different concentrations of ink.[6] Shortly after setting this system up, we found a steady flux of ink from one tank to the other. This state is not equilibrium—equilibrium requires that all fluxes equal *zero*. Nor is it truly steady—eventually the two tanks will reach equal concentrations, and the system does come to equilibrium with no net flux. Similarly, in the ratchet case the probability distribution $P(x,t)$ will come to a nearly time-indepedent form, as long as the external source of energy resetting the bolts remains available. The flux (net number of ratchets crossing $x = 0$ from left to right) need not be zero in this state.

To summarize, we have simplified our problem by arguing that we need only consider probability distributions $P(x,t)$ that are periodic in $x$ and independent of $t$. Our next step is to find an equation obeyed by $P(x,t)$, and solve it with these two conditions. To do so, we follow the derivation of the Nernst–Planck formula (see Equation 4.23 on page 126).

Note that in a time step $\Delta t$, each ratchet in our imagined collection gets a random thermal kick to the right or the left, in addition to the external applied force, just as in the derivation of Fick's law (Section 4.4.2 on page 115). Suppose first that there were no mechanical forces (no load and no bolts). Then we can just adapt the derivation leading to Equation 4.18 (compare Figure 4.10 on page 116):

- Subdivide each rod into imaginary segments of length $\Delta x$ much smaller than $L$.
- The distribution contains $MP(a)\Delta x$ ratchets located between $x = a - \frac{1}{2}\Delta x$ and $x = a + \frac{1}{2}\Delta x$. On average, half of these step to the right in time $\Delta t$.
- Similarly, there are $MP(a + \Delta x)\Delta x$ ratchets located between $x = a + \frac{1}{2}\Delta x$ and $x = a + \frac{3}{2}\Delta x$, of which half step to the *left* in time $\Delta t$.

[6] The concept of a quasi-steady, nonequilibrium state also entered the discussion of bacterial metabolism in Section 4.6.2. Sections 10.4.1 and 11.2.2 will again make use of this powerful idea.

- •Thus the net number of ratchets in the distribution crossing $x = a + \frac{1}{2}\Delta x$ from left to right is $\frac{1}{2}M[P(a) - P(a+\Delta x)]\Delta x \approx \frac{-(\Delta x)^2}{2} M \left.\frac{\mathrm{d}}{\mathrm{d}x}\right|_{x=a} P(x)$. (Here and below we drop terms of cubic and higher order in the small quantity $\Delta x$.)
- •We can compactly restate the last result as $-MD\frac{\mathrm{d}P}{\mathrm{d}x}\,\Delta t$, where $D$ is the diffusion constant for the movement of the ratchet along its axis in the surrounding viscous medium. (Recall $D = (\Delta x)^2/(2\Delta t)$ from Equation 4.5b on page 104).

Now we add the effect of an external force:

- Each ratchet also drifts under the influence of the force $-\frac{\mathrm{d}U_{\mathrm{tot}}}{\mathrm{d}x}$, where $U_{\mathrm{tot}}(x)$ is the potential energy function sketched in Figure 10.11c.
- The average drift velocity of those ratchets located at $x = a$ is $v_{\mathrm{drift}} = -\frac{D}{k_{\mathrm{B}}T} \left.\frac{\mathrm{d}}{\mathrm{d}x}\right|_{x=a} U_{\mathrm{tot}}$. (To get this expression, write the force as $-\mathrm{d}V_{\mathrm{tot}}/\mathrm{d}x$ and use the Einstein relation, Equation 4.15 on page 108, to express the viscous friction coefficient in terms of $D$.)
- The net number of ratchets crossing $x = a$ in time $\Delta t$ from the left thus gets a second contribution, $M \times P(a) v_{\mathrm{drift}} \Delta t$, or $-\frac{MD}{k_{\mathrm{B}}T} P \frac{\mathrm{d}U_{\mathrm{tot}}}{\mathrm{d}x}\,\Delta t$.

The arguments just given yielded two contributions to the number of systems crossing a given point in time $\Delta t$. Adding these contributions and dividing by $\Delta t$ gives:

$$j^{(1\mathrm{d})} \equiv \text{net number crossing per time} = -MD\Big(\frac{\mathrm{d}P}{\mathrm{d}x} + \frac{1}{k_{\mathrm{B}}T} P \frac{\mathrm{d}U_{\mathrm{tot}}}{\mathrm{d}x}\Big). \tag{10.3}$$

(In this one-dimensional problem the appropriate dimensions for a flux are $\mathbb{T}^{-1}$.) In order for the probability distribution $P(x)$ to be time-independent, we now require that probability is not piling up anywhere. This requirement means that the expression in Equation 10.3 must be independent of $x$. (A similar argument led us to the diffusion equation, Equation 4.19 on page 118.) In this context the resulting formula is called the **Smoluchowski equation**:

$$0 = \frac{\mathrm{d}}{\mathrm{d}x}\left(\frac{\mathrm{d}P}{\mathrm{d}x} + \frac{1}{k_{\mathrm{B}}T} P \frac{\mathrm{d}U_{\mathrm{tot}}}{\mathrm{d}x}\right). \tag{10.4}$$

**The equilibrium case** We want to find some periodic solutions to Equation 10.4 and interpret them. First suppose that the potential $U_{\mathrm{tot}}(x)$ is itself periodic: $U_{\mathrm{tot}}(x + L) = U_{\mathrm{tot}}(x)$. This situation corresponds to the unloaded G-ratchet (Figure 10.11a), or to the S-ratchet (Figure 10.11c) with $f = \epsilon/L$.

**Example**

Show that in this case the Boltzmann distribution is a solution of Equation 10.4, find the net probability per time to cross $x$, and explain why your result makes physical sense.

*Solution:* We expect that the system will just come to equilibrium, where it makes no net progress at all. Indeed, taking $P(x) = A\mathrm{e}^{-U_{\mathrm{tot}}(x)/k_{\mathrm{B}}T}$ gives a periodic, time-independent probability distribution. Equation 10.3 then gives that $j^{(1\mathrm{d})}(x) = 0$ everywhere. Hence this $P(x)$ is indeed a solution to the Smoluchowski equation with *no* net motion.

Since $j^{(1\mathrm{d})} = 0$, Sullivan's first claim was right (see page 365): The unloaded G-ratchet makes no net progress in either direction. We can also confirm Sullivan's physical reasoning for this claim: Indeed the function $\mathrm{e}^{-U_{\mathrm{tot}}(x)/k_{\mathrm{B}}T}$ peaks at the lowest-energy points, so each ratchet spends a lot of its time poised to hop *backward* whenever a chance thermal fluctuation permits this.

**Beyond equilibrium** The Boltzmann distribution only applies to systems at equilibrium. To tackle *non*equilibrium situations, begin with the "perfect ratchet" case (very large energy step $\epsilon$). We already encountered the perfect ratchet when deriving the estimate Equation 10.2. Thus, as soon as a ratchet arrives at one of the steps in the energy landscape, it immediately falls down the step and cannot return; the probability $P(x)$ is thus nearly zero just to the left of each step, as shown in Figure 10.12.

**Your Turn 10c**

Verify that the function $P(x) = A(\mathrm{e}^{-(x-L)f/k_\mathrm{B}T} - 1)$ vanishes at $x = L$, solves the Smoluchowski equation with the potential $V_\mathrm{tot}(x) = fx$, and resembles the curve sketched in Figure 10.12 between 0 and $L$. (Here $A$ is some positive constant.) Substitute into Equation 10.3 to find that $j^{(1\mathrm{d})}(x)$ is everywhere constant and positive.

You have just verified Sullivan's third claim (the loaded S-ratchet can indeed make net rightward progress), in the limiting case of a perfect ratchet. The constant $A$ should be chosen to make $P(x)\mathrm{d}x$ a properly normalized probability distribution, but we won't need its actual value. Outside the region between 0 and $L$, we make $P(x)$ periodic by just copying it (see Figure 10.12).

Let us find the average speed $v$ of the perfect S-ratchet. First we need to think about what $v$ means. Figure 10.12 shows the distribution of positions attained by a large collection of $M$ ratchets. Even though the populations at each position are assumed to be constant, there can be a net motion, just as we found when studying quasi-steady diffusion in a thin tube (Section 4.6.1 on page 121). To find this net motion, we count how many ratchets in the collection are initially located in a single period $(0, L)$, then find the average time $\Delta t$ it takes for all of them to cross the point $L$ from left to right, using the flux $j^{(1\mathrm{d})}$ found in Equation 10.3:

$$\Delta t = (\text{number})/(\text{number/time}) = \left(\int_0^L \mathrm{d}x\, MP(x)\right) \Big/ \left(j^{(1\mathrm{d})}\right). \tag{10.5}$$

Then the average speed $v$ is given by

$$v = L/\Delta t = \left(Lj^{(1\mathrm{d})}\right) \Big/ \left(M\int_0^L \mathrm{d}x\, MP(x)\right). \tag{10.6}$$

The normalization constant $A$ drops out of this result (and so does $M$).

Substituting the expressions in Your Turn 10c into Equation 10.5 gives

$$\Delta t = \frac{1}{Df/k_\mathrm{B}T} \int_0^L \mathrm{d}x \left(\mathrm{e}^{-(x-L)f/k_\mathrm{B}T} - 1\right),$$

or

$$\boxed{v = \left(\frac{fL}{k_\mathrm{B}T}\right)^2 \frac{D}{L}\left(\mathrm{e}^{fL/k_\mathrm{B}T} - 1 - fL/k_\mathrm{B}T\right)^{-1}. \qquad \text{speed of loaded, perfect S-ratchet}} \tag{10.7}$$

Although our answer is a bit complicated, it does have one simple qualitative feature: It's finite. That is, even though we took a very large energy step (the perfect ratchet case), the ratchet has a finite limiting speed.

**Your Turn 10d**

a. Show that in the case of *zero* external force Equation 10.7 reduces to $2D/L$, agreeing with our rough analysis of the unloaded perfect ratchet (Equation 10.2).

b. Show that at *high* force (but still much smaller than $\epsilon/L$), Equation 10.7 reduces to

$$\left(\frac{fL}{k_{\mathrm{B}}T}\right)^2 \frac{D}{L} \mathrm{e}^{-fL/k_{\mathrm{B}}T}. \tag{10.8}$$

The last result establishes Sullivan's fourth claim (forward stepping rate contains an exponential activation-energy factor), in the perfect-ratchet limit (backward stepping rate equals zero).

Though we only studied the perfect-ratchet limit, we can now guess what will happen more generally. Consider the equilibrium case, where $f = \epsilon/L$. At this point the activation barriers to forward and reverse motion are equal. Your result in Your Turn 10d(b) suggests that then the forward and reverse rates cancel, giving no net progress. This argument should sound familiar—it is just the kinetic interpretation of equilibrium (see Section 6.6.2 on page 194). At still greater force, $f > \epsilon/L$, the barrier to backward motion is actually smaller than the one for forward motion (see Figure 10.11d), and the machine makes net progress to the left. That was Sullivan's second claim.

**Summary** The S-ratchet makes progress to the right when $f \ll \epsilon/L$, then slows and reverses as we raise the load force beyond $f = \epsilon/L$.

The S-ratchet may seem rather artificial, but it illustrated some useful principles applicable to any molecular-scale machine:

1. Molecular-scale machines move by random-walking over their energy landscape, not by deterministic sliding.
2. They can pass through potential-energy barriers, with an average waiting time given by an exponential factor.
3. They can store potential energy (this is in part what creates the landscape), but not kinetic energy (since viscous dissipation is strong in the nanoworld, see Chapter 5).

Point (3) above stands in contrast to familiar macroscopic machines like a pendulum clock, whose rate is controlled by the inertia of the pendulum. Inertia is immaterial in the highly damped nanoworld; instead the speed of a molecular motor is controlled by activation barriers.

Our study of ratchets has also yielded some more specific results:

*a. A thermal machine can convert stored internal energy $\epsilon$ into directed motion, if it is constructed asymmetrically.*
*b. But structural asymmetry alone is not enough: A thermal machine won't go anywhere if it's in equilibrium (periodic potential, Figure 10.11a). To get useful work we must push it out of equilibrium, by arranging for a descending free energy landscape.*
*c. A ratchet's speed does not increase without bound as we increase the drive energy $\epsilon$. Instead, the speed of the unloaded ratchet saturates at some limiting value (Equation 10.7).* (10.9)

You showed in Your Turn 10d that with a load, the limiting speed gets reduced by an exponential factor relative to the unloaded $2D/L$. This result should remind you of the Arrhenius rate law (Section 3.2.4 on page 79). Chapter 3 gave a rather simpleminded approach to this law, imagining a single thermal kick carrying us all the way over a barrier. In the presence of viscous friction such

a one-kick passage may seem about as likely as a successful field goal in a football game played in molasses! But the Smoluchowski equation showed us the right way to derive the rate law for large molecules: Modeling the process as a random walk on an energy landscape gives qualitatively the same result as the naïve argument.

We could go on to implement these ideas for more complex microscopic machines, like the gears of Figure 10.6c. Rather than studying rolling on the potential energy surface (Figure 10.9 on page 362), we would set up a *two-dimensional* Smoluchowski equation on the surface, again arriving at conclusions similar to Idea 10.1. The following sections will not follow this program, however, instead seeking shortcuts to see the qualitative behavior without the difficult mathematics.

T2 *Section 10.2.3′ on page 398 generalizes the above discussion to get the force-velocity relation for an imperfect ratchet.*

## 10.3 Molecular implementation of mechanical principles

The discussion of purely mechanical machines in Section 10.2 generated some nice formulas, but still leaves us with many questions:

- Molecular-scale machines are presumably made of molecules, unlike the simple but rather fanciful sketches shown so far. Can we apply our ideas to single molecules?
- We still have no candidate model for a *cyclic* machine that eats *chemical* energy. Won't we need some totally new ideas to create this?
- Most important of all, how can we make contact with experimental data?

To make progress on the first question, it's time to gather a number of ideas about single molecules developed in previous chapters.

### 10.3.1 Three ideas

Here are some of those ideas.

First, the statistical physics of Chapter 6 was constructed to be applicable to single-molecule subsystems. For example, Section 6.6.3 on page 197 showed that such systems drive to minimize their free energy, just like macroscopic systems, though not necessarily in a one-way, deterministic fashion.

Second, we saw in Chapter 8 how chemical forces are nothing but changes in free energy, in principle interconvertible with other changes involving energy (for example, the release of the little bolts in the S-ratchet). Chemical forces drive a reaction in a direction determined by its $\Delta G$, a quantity involving the stoichiometry of the reaction but otherwise reflecting only the concentrations of molecules in the reservoir outside the reaction proper. We expressed this succinctly in Idea 8.22 on page 270, or in the slogan that "equilibrium doesn't care what happens inside the phone booth" (Section 8.2.2).

Third, Chapter 9 showed how even large, complex macromolecules, with tens of thousands of atoms all in random thermal motion, can nevertheless act as though they had just a few discrete states. Indeed macromolecules can snap crisply between those states, almost like a macroscopic light switch. We identified the source of this "multistable" behavior in the cooperative action of many weak physical interactions such as hydrogen bonds. Thus for example cooperativity made

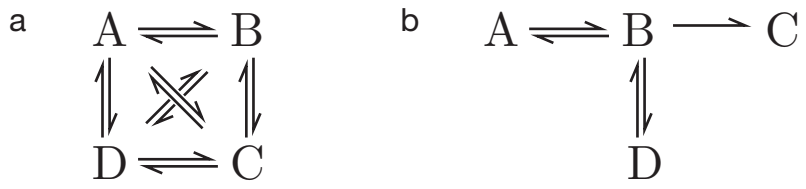


Figure 10.13: (Diagram.) (a) A fully connected reaction diagram. (b) A sparsely connected reaction diagram.

the helix–coil transition (Section 9.5.1), or the binding of oxygen by hemoglobin (Section 9.6.1) surprisingly sharp. Similarly, a macromolecule can be quite specific about what small molecules it binds, rejecting imposters by the cooperative effects of many charged or H-bonding groups in a precise geometrical arrangement (see Idea 7.17 on page 231).

### 10.3.2 The reaction coordinate gives a useful reduced description of a chemical event

The idea of multistability (the third point in Section 10.3.1), sometimes justifies us in writing extremely simple kinetic diagrams (or "reaction graphs") for the reactions of huge, complex macromolecules, as if they were simple molecules jumping between just a few well-defined configurations. The reaction graphs we write will consist of discrete symbols (or **nodes**) joined by arrows, just like many we have already written in Chapter 8, for example the isomerization reaction $A \rightleftharpoons B$ studied in Section 8.2.1. A crucial point is that such reaction graphs are in general **sparsely connected**. That is, many of the arrows one could imagine drawing between nodes will in fact be missing, reflecting the fact that the corresponding rates are negligibly small (Figure 10.13). Thus in many cases reactions can proceed only in sequential steps, rarely if ever taking shortcuts on the reaction graph. Usually we can't work out the details of the reaction graph from explicit calculations of molecular dynamics, but sometimes it's enough to frame guesses about a system from experience with similar systems, then look for quantitative predictions to test the guesses.

What exactly happens along those arrows in a reaction graph? To get from one configuration to the next, the atoms composing the molecule must rearrange their relative positions and angles. We could imagine listing the coordinates of every atom; then the starting and ending configurations are points on the many-dimensional space of these coordinates. In fact they are special points, for which the free energy is much lower than elsewhere. This property gives those points a special, nearly stable status, entitling them to be singled out as nodes on the reaction graph. If we could reach in and push individual atoms around, we'd have to do work on the molecule to move it away from either of these points. But we can instead wait for thermal motion to do the pushing for us:

> *Chemical reactions reflect random walks on an energy landscape in the space of molecular configurations.* (10.10)

Unfortunately the size of the molecular configuration space is daunting, even for small molecules. To get a tractable example, consider an ultra-simple reaction: A hydrogen atom, called $H_a$, collides with a hydrogen molecule, picking up one of the molecule's two atoms, $H_b$. To describe the spatial relation of the three H atoms, we can specify the three distances between pairs of atoms. Consider for example the configurations in which all three atoms lie on a single line, so that the two distances $d_{ab}$ and $d_{bc}$ fully specify the geometry. Then Figure 10.14 shows schematically the energy surface for

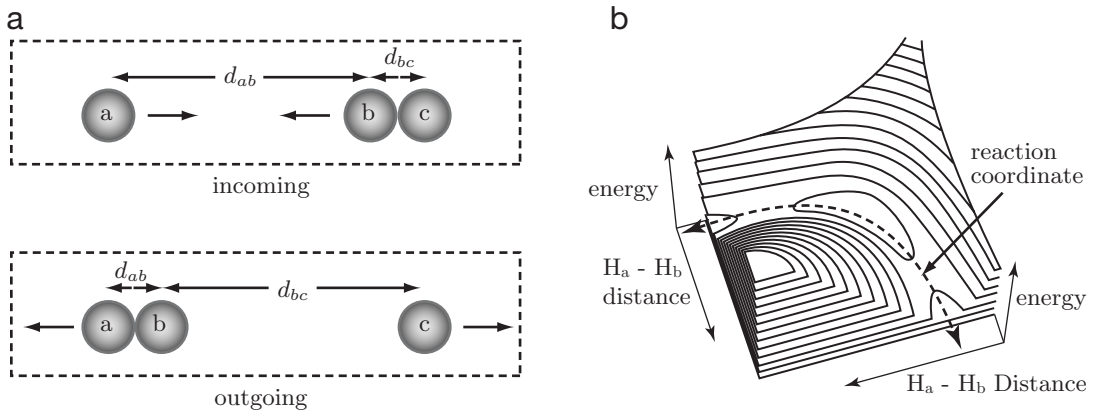


Figure 10.14: (Schematic; sketch graph.) (a) A simple chemical reaction: a hydrogen molecule transfers one of its atoms to a lone H atom, $H + H_2 \rightarrow H_2 + H$. (b) Imagined energy landscape for this reaction, assuming that the atoms travel on one straight line. The dashed line is the lowest path joining the starting and ending configurations shown in (a); it's like a path through a mountain pass. The reaction coordinate can be thought of as distance along this path. The highest point on this path is called the transition state.

the reaction. The energy is minimum at each end of the dashed line, where two H atoms are at the usual bond distance and the third is far away. The dashed line represents a path in configuration space that joins these two minima while climbing the energy landscape as little as possible. The barrier that must be surmounted in such a walk corresponds to the bump in the middle of the dashed line, representing an intermediate configuration with $d_{ab} = d_{bc}$.

When an energy landscape has a well-defined mountain pass, as in Figure 10.14, it makes sense to think of our problem approximately as just a one-dimensional walk *along this curve*, and to think in terms of the one-dimensional energy landscape seen along this walk. Chemists refer to the distance along the path as the **reaction coordinate**, and to the highest point along it as the **transition state**. We'll denote the height of this point on the graph by the symbol $G^\ddagger$.

Remarkably, the utility of the reaction coordinate idea has proven not to be limited to small, simple molecules. Even macromolecules described by thousands of atomic coordinates often admit a useful reduced description with just one or two reaction coordinates. Section 10.2.3 showed how the rate of barrier passage for a random walk on a one-dimensional potential is controlled by an Arrhenius exponential factor, involving the activation barrier; in our present notation this factor takes the form $e^{-G^\ddagger/k_B T}$. To test the idea that a given reaction is effectively a random walk on a one-dimensional free energy landscape, we write[7] $G^\ddagger/k_B T = (E^\ddagger/k_B T) - (S^\ddagger/k_B)$ Then our prediction is that the reaction rate should depend on temperature as

$$\text{rate} \propto e^{-E^\ddagger/k_B T}. \tag{10.11}$$

Indeed, many reactions among macromolecules obey such relations (see Figure 10.15). Section 10.3.3 will show how these ideas can help explain the enormous catalytic power of enzymes.

T2 *Section 10.3.2′ on page 399 gives some more comments about the energy landscape concept.*

[7] T2 More precisely, we should use the enthalpy in place of $E^\ddagger$.

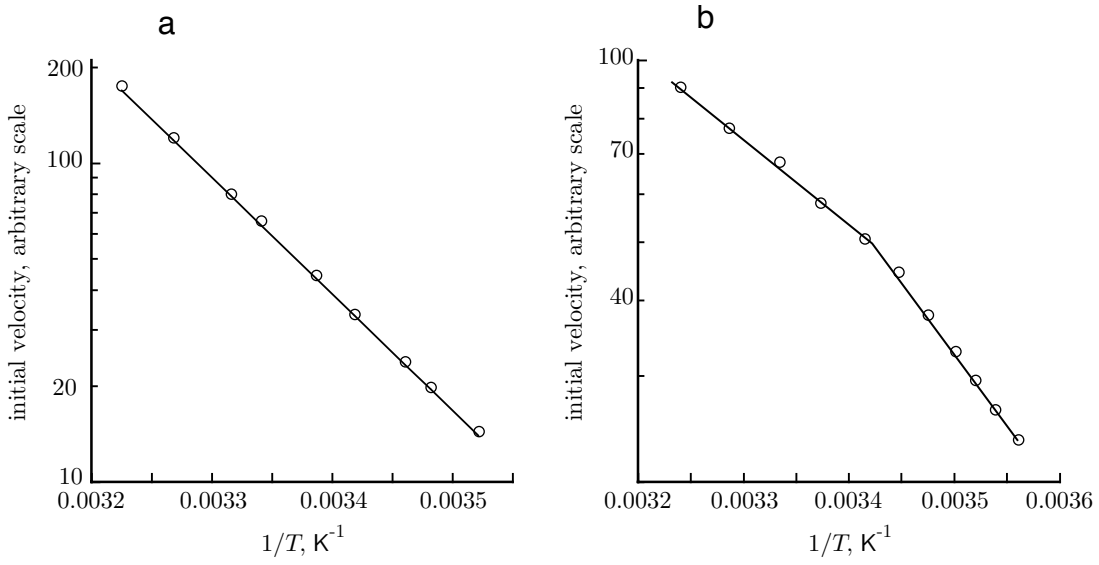


Figure 10.15: (Experimental data.) (a) Semilog plot of initial reaction velocity versus inverse temperature for the conversion of L-malate to fumarate by the enzyme , at pH 6.35. (b) The same for the reverse reaction. The first reaction follows the Arrhenius rate law (Equation 10.11), as shown by the straight line. The line is the function $\log_{10} v_0 = \text{const} - (3650\,\mathrm{K}/T)$, corresponding to an activation barrier of $29 k_B T_r$. The second reaction shows two different slopes; presumably an alternative reaction mechanism becomes available at temperatures above 294 K. [Data from Dixon & Webb, 1979.]

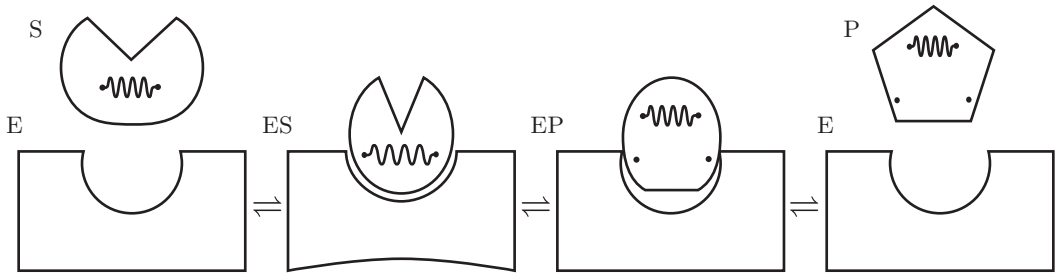


Figure 10.16: (Schematic.) Conceptual model of enzyme activity. (a) The enzyme E has a binding site with a shape and distribution of charges, hydrophobicity, and H-bonding sites approximately matching those presented by the substrate S. (b) To match perfectly, however, S (or both E and S) must deform. (Other, more dramatic conformational changes in the enzyme are possible too.) One bond in the substrate (shown as a spring in S) stretches close to its breaking point. (c) From the ES state, then, a thermal fluctuation can readily break the stretched bond, giving rise to the EP complex. A new bond can now form (upper spring), stabilizing the product P. (d) The P state is not a perfect fit to the binding site either, so it readily unbinds, returning E to its original state.

### 10.3.3 An enzyme catalyzes a reaction by binding to the transition state

Reaction rates are controlled by activation barriers, with a temperature dependence given roughly by an Arrhenius exponential factor (see Section 3.2.4 on page 79). Enzymes increase reaction rates, but maintain that characteristic temperature dependence (Figure 10.15). Thus it's reasonable to guess that *enzymes work by reducing the activation barrier to a reaction.* What may not be so clear is *how* they could accomplish such a reduction.

Figure 10.16 summarizes a mechanism proposed by J. Haldane in 1930. Using the mechanical

language of this chapter, let us imagine a substrate molecule S as an elastic body, with one particular chemical bond of interest shown in the figure as a spring. The substrate wanders at random until it encounters an enzyme molecule E. The enzyme molecule has been designed with a binding site whose shape is almost, but not quite, complementary to that of S. The site is assumed to be lined with groups that could make energetically favorable contacts with S (hydrogen bonds, electrostatic attractions, and so on), if only the shapes matched precisely.

Under these circumstances E and S may be able to lower their total free energy by deforming their shapes, in order to make close contact and profit from the many weak physical attractions at the binding site.[8] In Haldane's words, E. Fischer's famous lock-and-key metaphor should be amended to allow that "the key does not fit the lock quite perfectly, but rather exercises a certain strain on it." We will call the bound complex ES. But the resulting deformation on the particular bond of interest may push it closer to its breaking point, or in other words reduce its activation barrier to breaking. Then ES will isomerize to a bound state of enzyme plus product, or EP, much more rapidly than S would spontaneously isomerize to P. If the product is also not a perfect fit to the enzyme's binding site, it can then readily detach, leaving the enzyme in its original state. Each step in the process is reversible; the enzyme also catalyzes the reverse reaction P $\rightarrow$ S (see Figure 10.15).

Let us see how the events in the little story above actually amount to a reduction in activation energy. Figure 10.17a sketches an imagined free energy landscape for a single molecule S to isomerize (convert) spontaneously to P (top curve). The geometric change needed to make S fit the binding site of E is assumed to carry S along its reaction coordinate, with the tightest fit at the transition state $S^{\ddagger}$. The enzyme may also change its conformation to one different from its usual (lowest free energy) state (lower curve). These changes increase the self-energies of E and S, but they are partially offset by a sharp *de*crease in the interaction (or binding) energy of the complex ES (middle curve). Adding the three curves gives a total free energy landscape with a reduced activation barrier to the formation of the transition state $ES^{\ddagger}$ (Figure 10.17b).

The picture outlined in the preceding paragraph should not be taken too literally. For example, there's really no unambiguous way to divide the free energy into the three separate contributions shown in Figure 10.17a. Nevertheless, the conclusion is valid:

> *Enzymes work by reducing the activation energy for a desired reaction. To bring about this reduction, the enzyme is constructed to bind most tightly to the substrate's transition state.* (10.12)

In effect, the enzyme-substrate complex *borrows* some of the free energy needed to form the transition state from the many weak interactions between the substrate and the enzyme's binding site. This borrowed energy must be paid back when the product unbinds, in order to return the enzyme to its original state. Thus

> *An enzyme cannot alter the net $\Delta G$ of the reaction.* (10.13)

An enzyme speeds up *both* the forward and backward reactions; the direction actually chosen is still determined by $\Delta G$, a quantity external to the enzyme, as always (see Idea 8.14 on page 267).

Up to this point we have been imagining a system containing just one molecule of substrate. With a simple modification, however, we can now switch to thinking of our enzyme as a *cyclic*

[8] Other kinds of deformations are possible besides shape changes, for example charge rearrangements. This chapter uses mechanical ideas like shape change as metaphors for all sorts of deformations.

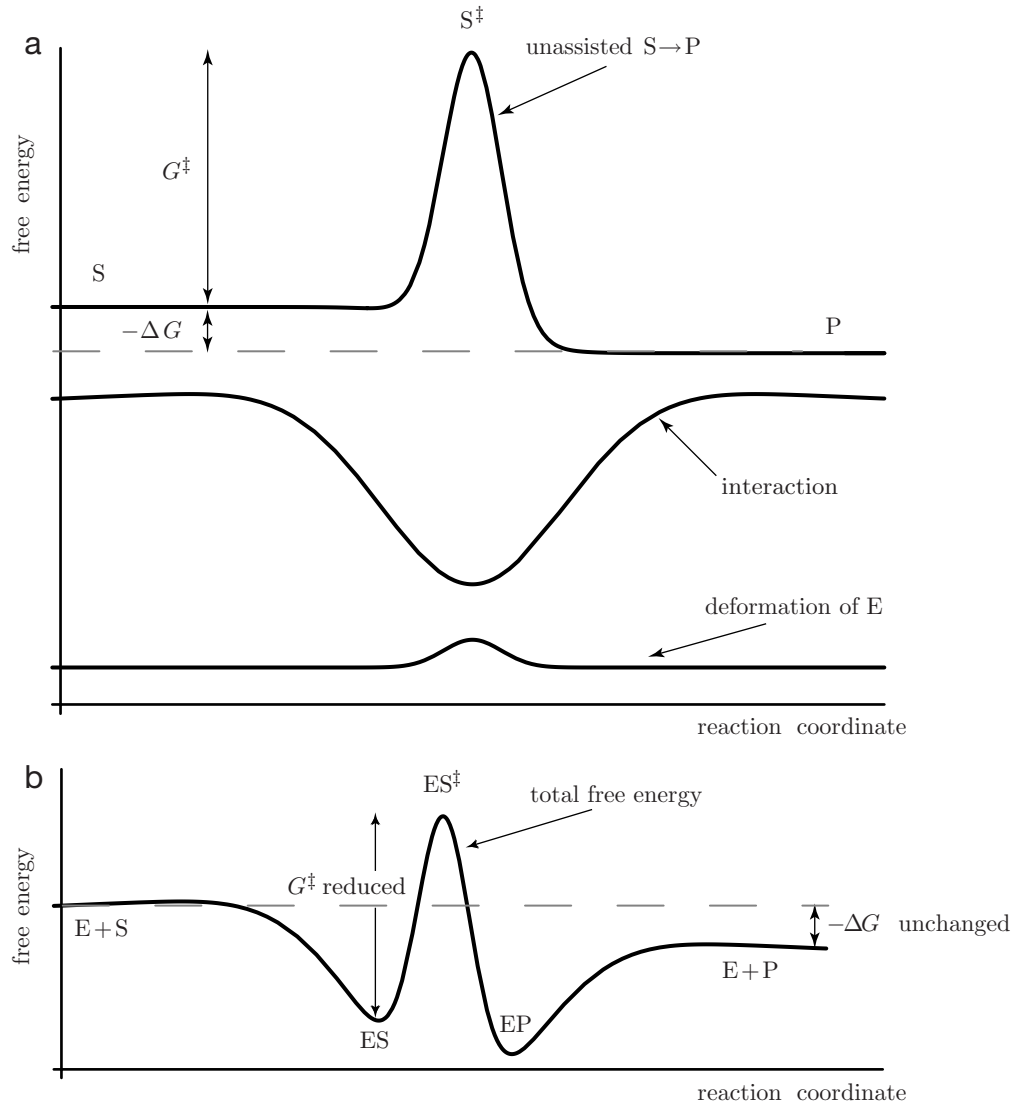


Figure 10.17: (Sketch graphs.) (a) Imagined free energy landscapes corresponding to the story line in Figure 10.16. *Top curve:* The substrate S can spontaneously convert to P only by surmounting a large activation barrier $G^{\ddagger}$, the free energy of the transition state $S^{\ddagger}$ relative to S. *Middle curve:* the interaction free energy between substrate and product includes a large binding free energy (dip), as well as the entropic cost of aligning the substrate properly relative to the enzyme (slight bumps on either side of the dip). *Lower curve:* The binding free energy may be partly offset by a deformation of the enzyme upon binding, but still the net effect of the enzyme is to reduce the barrier $G^{\ddagger}$. All three curves have been shifted by arbitrary constants in order to show them on a single set of axes. (b) Imagined net free energy landscape obtained by summing the three curves in (a). The enzyme has reduced $G^{\ddagger}$, but it cannot change $\Delta G$.

*machine*, progressively processing a large batch of S molecules. When many molecules of S are available, then the net driving force for the reaction includes an entropic term of the form $k_{\mathrm{B}}T \ln c_{\mathrm{S}}$, where $c_{\mathrm{S}}$ is the concentration. (See Equation 8.3 on page 261 and Equation 8.13 on page 267.) The effect of a high concentration of S, then, is to pull the left end of the free-energy landscape (Figure 10.17b) upward, reducing or eliminating any activation barrier to the formation of the complex ES and thus speeding up the reaction. Similarly, an increase in $c_{\mathrm{P}}$ pulls up the right end

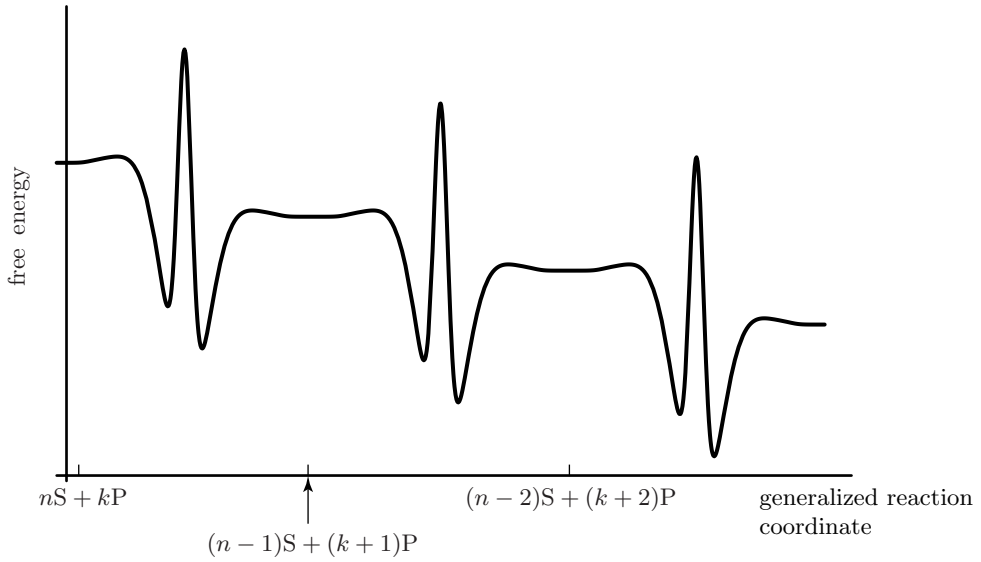


Figure 10.18: (Sketch graph.) The free energy landscape of Figure 10.17b, duplicated and shifted to show three steps in a cyclic reaction. The reaction coordinate of Figure 10.17 has been generalized to include changes in the number of enzyme and substrate molecules; the curve shown connects the state with $n$ substrate and $k$ product molecules to the state with three fewer S (and three more P).

of the free energy landscape, slowing or halting the unbinding of product. Just as in any chemical reaction, a large enough concentration of P can even reverse the sign of $\Delta G$, and hence reverse the direction of the net reaction (see Section 8.2.1).

We can now make a simple but crucial observation: The state of our enzyme/substrate/product system depends on how many molecules of S have been processed into P. Although the enzyme returns to its original state after one cycle, still the whole system's free energy falls by $\Delta G$ every time it takes one net step. We can acknowledge this fact by generalizing the reaction coordinate to include the progress of the reaction, for example the number $N_S$ of remaining substrate molecules. Then *the complete free-energy landscape consists of many copies of Figure 10.17b, each shifted downward by $\Delta G$ so as to make a continuous curve* (Figure 10.18). In fact, this curve looks qualitatively like one we already studied, namely Figure 10.11c! We identify the barrier $fL$ in that figure as $G^\ddagger$, and the net drop $fL - \epsilon$ as $\Delta G$. In short,

> *Many enzymes can be regarded as simple cyclic machines; they work by random-walking down a one-dimensional free energy landscape. The net descent of this landscape in one forward step is the value of $\Delta G$ for the reaction S⇀P.* (10.14)

Idea 10.14 gives an immediate qualitative payoff: We see at once why so many enzymes exhibit saturation kinetics (Section 10.1.2). Recall what this means. The rate of an enzyme-catalyzed reaction S⇀P typically levels off at high concentration of S, instead of being proportional to $c_S$ as simple collision theory might have led us to expect. Viewing enzyme catalysis as a walk on a free energy landscape shows that saturation kinetics is a result we've already obtained, namely our result for the speed of a perfect ratchet (Idea 10.9c on page 369). A large concentration of S pulls the left side of the free energy landscape upward. This means that the step from E+S to ES in Figure 10.17b is steeply downhill. Such a steep downward step makes the process effectively irreversible, essentially forbidding backward steps, but it doesn't speed up the net progress, as seen

in the analysis leading to Equation 10.7 on page 368. That's because eliminating the first bump in Figure 10.17b doesn't affect the *middle* bump. Indeed the activation barrier to pass from ES to EP is insensitive to the availability of S, because the binding site is already occupied throughout this process.

We also see another way to make the catalytic cycle essentially irreversible: Instead of raising $c_S$, we can *lower* $c_P$, pulling the *right* side of the landscape steeply *down*. It makes sense—if there's no product, then the rate for E to bind P and convert it to S will be zero! Section 10.4 below will turn all these qualitative observations into a simple, quantitative theory of enzyme catalysis rates, then apply the same reasoning to molecular machines.

Idea 10.14 also yields a second important qualitative prediction. Suppose we find another molecule $\widetilde{S}$ similar to S, but whose relaxed state resembles the stretched (transition) state of S. Then we may expect that $\widetilde{S}$ will bind to E even more tightly than S itself, since it gains the full binding energy without having to pay any elastic-strain energy. L. Pauling suggested in 1948 that introducing even a small amount of such a **transition state analog** $\widetilde{S}$ into a solution of E and S would *poison* the enzyme: E will bind $\widetilde{S}$ tightly, and instead of catalyzing a change in $\widetilde{S}$ will simply hold on to it. Indeed today's protease inhibitors for the treatment of HIV infection were created by seeking transistion state analogs directed at the active site of the HIV protease enzyme.

T2 *Section 10.3.3′ on page 400 mentions other physical mechanisms that enzymes can use to facilitate reactions.*

### 10.3.4 Mechanochemical motors move by random-walking on a two-dimensional landscape

Idea 10.14 has brought chemical devices (enzymes) into the same conceptual framework as the microscopic mechanical devices studied in Section 10.2.2. This picture also lets us imagine how *mechano*chemical machines might work. Consider an enzyme that catalyzes the reaction of a substrate at high chemical potential, $\mu_S$, yielding a product with low $\mu_P$. In addition, this enzyme has a second binding site, which can attach it to any point of a periodic "track." This situation is meant as a model of a motor like kinesin (see Section 10.1.3), which converts ATP to ADP plus phosphate and can bind to periodically spaced sites on a microtubule.

The system just described has *two* markers of net progress, namely the number of remaining substrate molecules and the spatial location of the machine along its track. Taking a step in either of these two directions will in general require surmounting some activation barrier; for example, stepping along the track involves first unbinding from it. To describe these barriers, we introduce a two-dimensional free energy landscape, conceptually similar to Figure 10.8. Let $\beta$ denote the spatial position of one particular atom on the motor. Imagine holding $\beta$ fixed with a clamp, then finding the easiest path through the space of conformations at fixed $\beta$ that accomplishes one catalytic step; this gives a slice of the free energy landscape along a line of fixed $\beta$. Putting these slices together could in principle give the two-dimensional landscape.

If no external force acts on the enzyme, and if the concentrations of substrate and product correspond to thermodynamic equilibrium ($\mu_S = \mu_P$), then we get a picture like Figure 10.8a, and no net motion. If, however, there is are net chemical and mechanical forces, then we instead get a tilted landscape like Figure 10.9, and the enzyme will move, exactly as in Section 10.2.2! The

diagonal valleys in the landscape of Figure 10.9 implement the idea of a mechanochemical cycle:

> *A mechanochemical cycle amounts to a free-energy landscape with directions corresponding to reaction coordinate and spatial displacement. If the landscape is not symmetric under reflection in the mechanical ($\beta$) direction, and the concentrations of substrate and product are out of equilibrium, then the cycle can yield directed net motion.* (10.15)

This result is just a restatement of Ideas 10.9a,b on page 369.

Figure 10.9 on page 362 represents an extreme form of mechanochemical coupling, called **tight coupling**, in which a step in the mechanical ($\beta$) direction is nearly always linked to a step in the chemical ($\alpha$) direction. There are well-defined valleys, well separated by large barriers, and so very little hopping takes place from one valley to the next. In such a situation it makes sense to eliminate altogether the direction perpendicular to the valleys, just as we already eliminated the many other configurational variables (Figure 10.14b). Thus, we can imagine reducing our description of the system to a *single* reaction coordinate describing the location along just one of the valleys. With this simplification, our motor becomes simple indeed: It's just another one-dimensional device, with a free energy landscape resembling the S-ratchet (Figure 10.11c on page 364).

We must keep in mind that tight coupling is just a hypothesis to be checked; indeed Section 10.4.4 will argue that tight coupling is not necessary for a motor to function usefully. Nevertheless, for now let us keep the image of Figure 10.9 in mind as our provisional, intuitive notion of how coupling works.

## 10.4 Kinetics of real enzymes and machines

Certainly real enzymes are far more complicated than the sketches in the preceding sections might suggest. Figure 10.19 shows phosphoglycerate kinase, an enzyme playing a role in metabolism. (Chapter 11 will discuss the glycolysis pathway, to which this enzyme contributes.) The enzyme binds to phosphoglycerate (a modified fragment of glucose) and transfers its phosphate group to an ADP molecule, forming ATP. If the enzyme were instead to bind phosphoglycerate and a *water* molecule, the phosphate could be transferred to the water, and no ATP would be made. The kinase enzyme is beautifully designed to solve this engineering problem. It is composed of two domains connected by a flexible hinge. Some of the amino acids needed for the reaction are in its upper half, some in the lower half. When the enzyme binds to phosphoglycerate and ADP, the energy of binding these substrate molecules causes the enzyme to close around them. Only then are all of the proper amino acids brought into position, and inside, sheltered from water by the enzyme, the reaction is consummated.

In short, phosphoglycerate kinase is complex because it must not only channel the flow of probability for molecular states into a useful direction, but also *prevent* probability from flowing into *useless* processes. Despite this complexity, we can still see from its structure some of the general themes outlined in the preceding subsections. The enzyme is much larger than its two substrate binding sites; it grips the substrates in a close embrace, making many weak physical bonds; optimizing these physical bonds constrains the substrates to a precise configuration, presumably corresponding to the transition state for the desired phosphate transfer reaction.

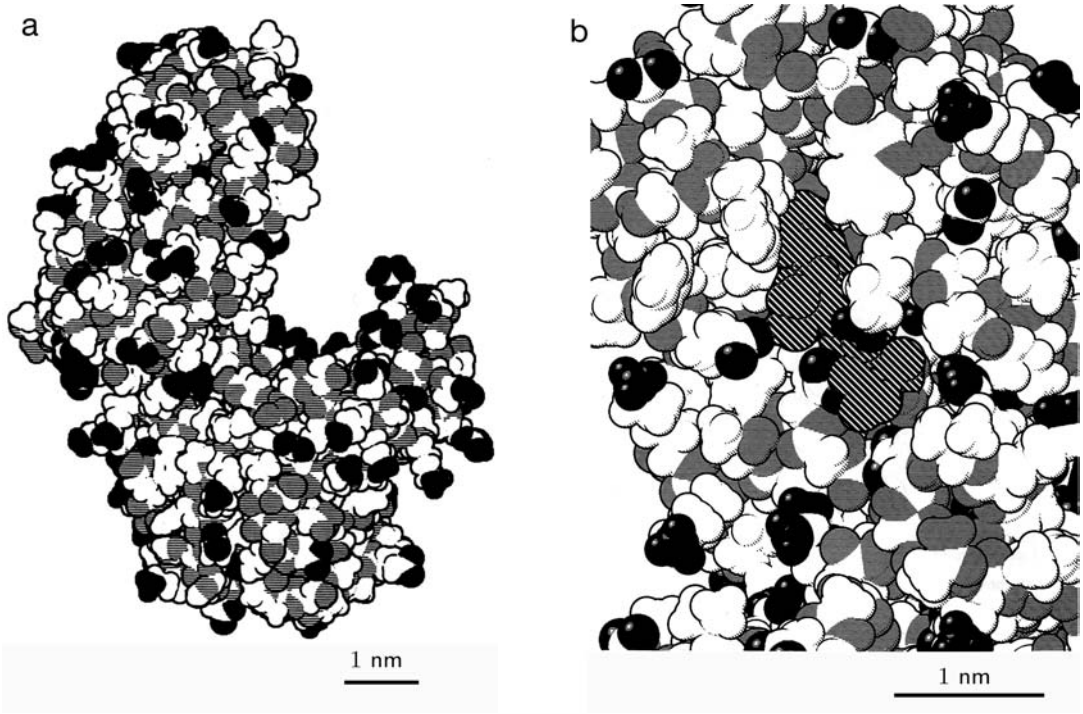


Figure 10.19: (Structure drawn from atomic coordinates.) (a) Structure of phosphoglycerate kinase, an enzyme composed of one protein chain of 415 amino acids. The chain folds into this distinctive shape, with two large lobes connected by a flexible hinge. The active site, where the chemical reaction occurs, is located between the two halves. The atoms are shown in a gray scale according to their hydrophobicity, with the most hydrophobic in white, the most hydrophilic in black. (b) Close-up of (a), showing the active site with a bound molecule of ATP (hatched atoms). This view is looking from the right in (a), centered on the upper lobe. Amino acids from the enzyme wrap around and hold the ATP molecule in a specific position. [From Goodsell, 1993.]

### 10.4.1 The Michaelis–Menten rule describes the kinetics of simple enzymes

**The MM rule** Section 10.2.3 gave us some experience calculating the net rate of a random walk down a free-energy landscape. We saw that such calculations boil down to solving the Smoluchowski equation (Equation 10.4 on page 367) to find the appropriate quasi-steady state. However, we generally don't know the free-energy landscape. Even if we did, such a detailed analysis focuses on the specifics of one enzyme, whereas we would like to begin by finding some very broadly applicable lessons. Let's instead take an extremely reductionist approach.

First, focus on a situation where initially there is no product present, or hardly any. Then the chemical potential $\mu_P$ of the product is a large negative number. This in turn means that the third step of Figure 10.17b, EP→E+P, is steeply downhill, and so we may treat this step as one-way forward—a perfect ratchet. We also make a related simplifying assumption, that the transition EP→E+P is so rapid that we may neglect EP altogether as a distinct step, lumping it together with E+P. Finally, we assume that the remaining quasi-stable states, E+S, ES, and E+P, are well separated by large barriers, so that each transition may be treated independently. Thus the transition involving binding of substrate from solution will also be supposed to proceed at a rate given by a first-order rate law, that is, the rate is proportional to the substrate concentration $c_S$ (see Section 8.2.3).

Now suppose we throw a single enzyme molecule into a vat initially containing substrate at concentration $c_{\mathrm{S,i}}$ and a negligible amount of product.[9] This system is far from equilibrium, but it soon comes to a quasi-steady state: The concentration of substrate remains nearly constant, and that of product nearly zero, since substrate molecules enormously outnumber the one enzyme. The enzyme spends a certain fraction $P_{\mathrm{E}}$ of its time unoccupied, and the rest, $P_{\mathrm{ES}} = 1 - P_{\mathrm{E}}$ bound to substrate, and these numbers too are nearly constant in time. Thus the enzyme converts substrate at a constant rate, which we'd like to find.

Let us summarize the discussion so far in a reaction formula:

$$\mathrm{E} + \mathrm{S} \underset{k_{-1}}{\overset{k_1}{\rightleftharpoons}} \mathrm{ES} \overset{k_2}{\rightharpoonup} \mathrm{E} + \mathrm{P}. \tag{10.16}$$

It's a cyclic process: The starting and ending states in this formula are different, but in each the enzyme itself is in the same state. The notation associates rate constants to each process (see Section 8.2.3 on page 269). We are considering only one molecule of E; thus the rate of conversion for E+S⇀ES is $k_1 c_{\mathrm{S}}$, not $k_1 c_{\mathrm{S}} c_{\mathrm{E}}$.

In a short time interval $\mathrm{d}t$, the probability $P_{\mathrm{E}}$ to be in the state E can change in one of three ways:

1. If the enzyme is initially in the unbound state E, it has probability per unit time $k_1 c_{\mathrm{S}}$ of binding substrate and hence leaving the state E.
2. If the enzyme is initially in the enzyme-substrate complex state ES, it has probability per unit time $k_2$ of processing and releasing product, hence reentering the unbound state E.
3. The enzyme-substrate complex also has probability per unit time $k_{-1}$ of losing its bound substrate, reentering the state E.

Expressing the above argument in a formula (see Idea 6.29 on page 196),

$$\frac{\mathrm{d}}{\mathrm{d}t} P_{\mathrm{E}} = -k_1 c_{\mathrm{S}} \times (1 - P_{\mathrm{ES}}) + (k_{-1} + k_2) \times P_{\mathrm{ES}}. \tag{10.17}$$

Make sure you understand the units on both sides of this formula.

The quasi-steady state is the one for which Equation 10.17 equals zero. Solving gives the probability to be in the state ES as

$$P_{\mathrm{ES}} = \frac{k_1 c_{\mathrm{S}}}{k_{-1} + k_2 + k_1 c_{\mathrm{S}}}. \tag{10.18}$$

According to Equation 10.16, the rate at which a single enzyme molecule creates product is Equation 10.18 times $k_2$. Multiplying by the concentration $c_{\mathrm{E}}$ of enzyme then gives the reaction velocity $v$, defined in Section 10.1.2.

The preceding paragraph outlined how to get the initial reaction velocity as a function of the initial concentrations of enzyme and substrate, for a reaction with an irreversible step (Reaction 10.16). We can tidy up the formula by defining the **Michaelis constant** $K_{\mathrm{M}}$ and maximum velocity $v_{\max}$ of the reaction to be

$$K_{\mathrm{M}} \equiv (k_{-1} + k_2)/k_1 \quad \text{and} \quad v_{\max} \equiv k_2 c_{\mathrm{E}}. \tag{10.19}$$

[9] Even if there are many enzyme molecules, we can expect the same calculations to hold as long as their concentration is much smaller than that of substrate.

Thus $K_M$ has the units of a concentration; $v_{max}$ is a rate of change of concentration. In terms of these quantities, Equation 10.18 becomes the **Michaelis–Menten** (or **MM**) **rule**:

$$\boxed{v = v_{max}\frac{c_S}{K_M + c_S}. \qquad \text{Michaelis–Menten rule}} \tag{10.20}$$

The MM rule displays saturation kinetics. At very low substrate concentration the reaction velocity is proportional to $c_S$, as we might have expected from naïve one-step kinetics (Section 8.2.3 on page 269). At higher concentration, however, the extra delay in escaping from the enzyme-substrate complex starts to modify that result: $v$ continues to increase with increasing $c_S$, but never exceeds $v_{max}$.

Let us pause to interpret the two constants $v_{max}$ and $K_M$ describing a particular enzyme. The maximum turnover number $v_{max}/c_E$, defined in Section 10.1.2, reflects the intrinsic speed of the enzyme. According to Equation 10.19, this quantity just equals $k_2$, which is indeed a property of a single enzyme molecule. To interpret $K_M$, we first notice that when $c_S = K_M$ then the reaction velocity is just one half of its maximum. Suppose the enzyme binds substrate rapidly relative to the rate of catalysis and the rate of substrate dissociation (that is, suppose $k_1$ is large). Then even a low value of $c_S$ will suffice to keep the enzyme fully occupied, or in other words $K_M$ will be small. The explicit formula (Equation 10.19) confirms this intuition.

**The Lineweaver–Burk plot** Our very reductionist model of a catalyzed reaction has yielded a testable result: We claim to predict the full dependence of $v$ upon $c_S$, a *function*, using only two phenomenological fitting parameters, $v_{max}$ and $K_M$. An algebraic rearrangement of the result shows how to test whether a given experimental dataset follows the Michaelis–Menten rule. Instead of graphing $v$ as a function of $c_S$, consider graphing the reciprocal $1/v$ as a function of $1/c_S$ (a "**Lineweaver–Burk plot**"). Equation 10.20 then becomes

$$\frac{1}{v} = \frac{1}{v_{max}}\left(1 + \frac{K_M}{c_S}\right). \tag{10.21}$$

That is, the MM rule predicts that $1/v$ should be a linear function of $1/c_S$, with slope $K_M/v_{max}$ and intercept $1/v_{max}$.

Remarkably, many enzyme-mediated reactions really do obey the MM rule, even though few are so simple as to satisfy our assumptions literally.

**Example**

Pancreatic carboxypeptidase cleaves amino acid residues from one end of a polypeptide. The table below gives the initial reaction velocity versus $c_S$ for this reaction for a model system, a peptide of just two amino acids :

| Substrate concentration (mM) | 2.5 | 5.0 | 10.0 | 15.0 | 20.0 |
|---|---|---|---|---|---|
| Initial velocity ($\mathrm{mM\,s^{-1}}$) | 0.024 | 0.036 | 0.053 | 0.060 | 0.064 |

Find $K_M$ and $v_{max}$ by the Lineweaver–Burk method and verify that this reaction obeys the MM rule.

*Solution:* The graph in Figure 10.20b is indeed a straight line, as expected from the MM rule. Its slope equals 75 s, and the intercept is $12\,\mathrm{mM^{-1}\,s}$. From the above formulas, then, $v_{max} = 0.085\,\mathrm{mM\,s^{-1}}$ and $K_M = 6.4\,\mathrm{mM}$.

The key to the great generality of the MM rule is that some of the assumptions we made were not necessary. Problem 10.6 illustrates the general fact that *any* one-dimensional device (that is, one

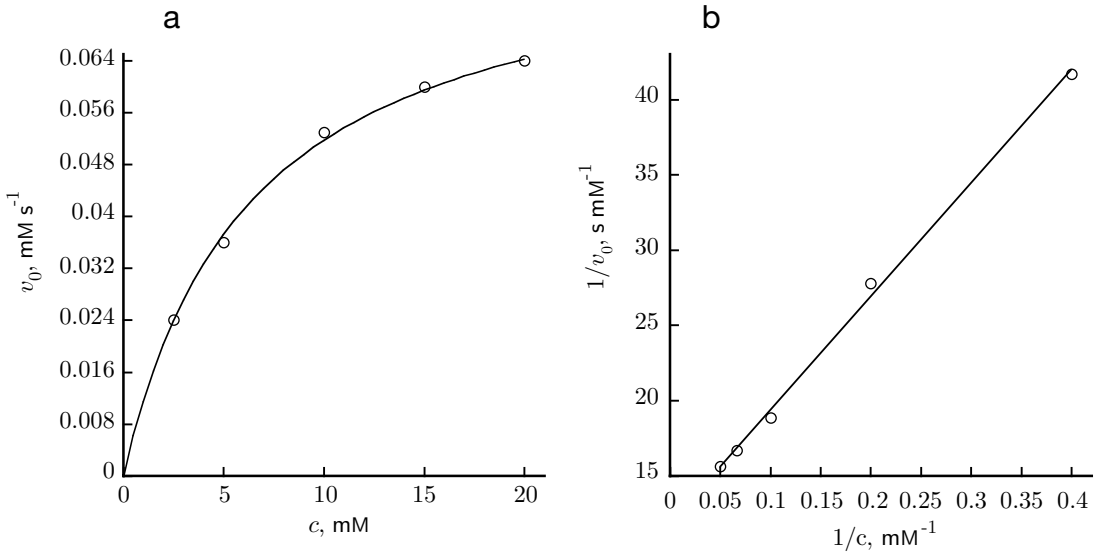


Figure 10.20: (Experimental data.) (a) Reaction velocity versus substrate concentration for the reaction catalyzed by pancreatic carboxypeptidase (see the Example on page 381). (b) The same data, plotted in the Lineweaver–Burk form (see Equation 10.21). [Data from Lumry et al., 1951.]

with a linear sequence of steps) effectively gives rise to a rate law of the form Equation 10.20, as long as the last step is irreversible.

### 10.4.2 Modulation of enzyme activity

Enzymes create and destroy molecular species. To keep everything working, the cell must regulate these activities. One strategy involves regulating the rate at which an enzyme is itself created, by regulating the gene coding for it (see Section 2.3.3 on page 57). For some applications, however, this strategy is not fast enough; instead the cell regulates the turnover numbers of the existing enzyme molecules. For example, an enzyme's activity may be slowed by the presence of another molecule that binds to, or otherwise directly interferes with, its substrate binding site ("competitive inhibition"; see Problem 10.4). Or a control molecule may bind to a second site on the enzyme, altering activity at the substrate site by an allosteric interaction ("noncompetitive inhibition"; see Problem 10.5). One particularly elegant arrangement is when a chain of enzymes synthesizes a product, and the first in the chain is inhibited by the presence of the final product itself, a feedback loop (see Figure 9.10 on page 331).

### 10.4.3 Two-headed kinesin as a tightly coupled, perfect ratchet

Section 10.3.4 suggested that the kinetics of a tightly coupled molecular motor would be much the same as those of an enzyme. In the language of free energy landscapes (Figure 10.9 on page 362), this means that we expect to find a one-dimensional random walk down a single valley, corresponding to the successive processing of substrate to product (shown as motion toward negative values of $\alpha$), combined with successive spatial steps (shown as motion toward negative values of $\beta$). If the concentration of product is kept very low, then the random walk along $\alpha$ will have an irreversible step, and hence so will the overall motion along the valley. We therefore expect that the analysis

of Section 10.4.1 should apply, with one modification: Since the average rate of stepping depends on the free energy landscape along the valley, in particular it will depend on the applied load force (the tilt in the $\beta$ direction), just as in Sections 10.2.1–10.2.3. In short, then, we expect that

> *A tightly coupled molecular motor, with at least one irreversible step in its kinetics, should move at a speed governed by the Michaelis–Menten rule, with parameters $v_{\max}$ and $K_M$ dependent upon the load force.* (10.22)

A real molecular motor will, however, have some important differences from the "bumpy rubber gears" imagined in Section 10.2.1. One difference is that we expect an enzyme's free energy landscape to be even more rugged than the one shown in Figure 10.9. Activation barriers will give the most important limit on the rate of stepping, not the viscous friction imagined in Section 10.2.1. In addition, we have no reason to expect that the valleys in the energy landscape will be the simple diagonals imagined in Figure 10.9. More likely, they will zigzag from one corner to the other. Some substeps may follow a path nearly parallel to the $\alpha$-axis (a "purely chemical step"). The landscape along such a substep is unaffected by tilting in the $\beta$ direction, so its rate will be nearly independent of the applied load. Other substeps will follow a path at some angle to the $\alpha$-axis (a "mechanochemical step"); their rate will be sensitive to load.

Physical measurements can reveal details about the individual kinetic steps in a motor's operation. This section will follow an analysis due to M. Schnitzer, K. Visscher, and S. Block. Building on others' ideas, these authors argued for a model of kinesin's cycle similar to the one sketched in Figure 10.21. The rest of this section will outline the evidence leading to this model and describe the steps symbolized by the cartoons in the figure.

**Clues from kinetics** Conventional (or "two-headed") kinesin forms a "homodimer," an association of two identical protein subunits. This structure lets kinesin walk along its microtubule track with a **duty ratio** of nearly 100%. The duty ratio is the fraction of the total cycle during which the motor is bound to its track, and cannot slide freely along it; a high duty ratio lets the motor move forward efficiently even when an opposing load force is applied. One way for kinesin to achieve its high duty ratio could be by coordinating the detachment of its two identical heads in a "hand-over-hand" manner, so that at any moment one is always attached while the other is stepping.[10]

Kinesin is also highly **processive**. That is, it takes many steps (typically about one hundred) before detaching from the microtubule. Processivity is a very convenient property for the experimentalist seeking to study kinesin. Thanks to processivity, it's possible to follow the progress of a micron-size glass bead for many steps as it is hauled along a microtubule by a single kinesin molecule. Using optical tweezers and a feedback loop, experimenters can also apply a precisely known load force to the bead, then study the kinetics of kinesin stepping at various loads.

K. Svoboda and coauthors initiated a series of single-molecule motility assays of the type just described in 1993. Using an interferometry technique, they resolved individual steps of a kinesin dimer attached to a bead of radius 0.5 $\mu$m, finding that each step was 8 nm long, exactly the distance between successive kinesin binding sites on the microtubule track (see Figure 10.22). Moreover, as shown in the figure, kinesin rarely takes backward steps, even under a significant backward load force: In the terminology of Section 10.2.3, it is close to the "perfect ratchet" limit.

[10] T2 Recent work has cast doubt on the hand-over-hand picture, in which the two kinesin heads execute identical chemical cycles (see Hua et al., 2002). Whatever the final model of kinesin stepping may be, however, it will have to be consistent with the experiments discussed in this section.

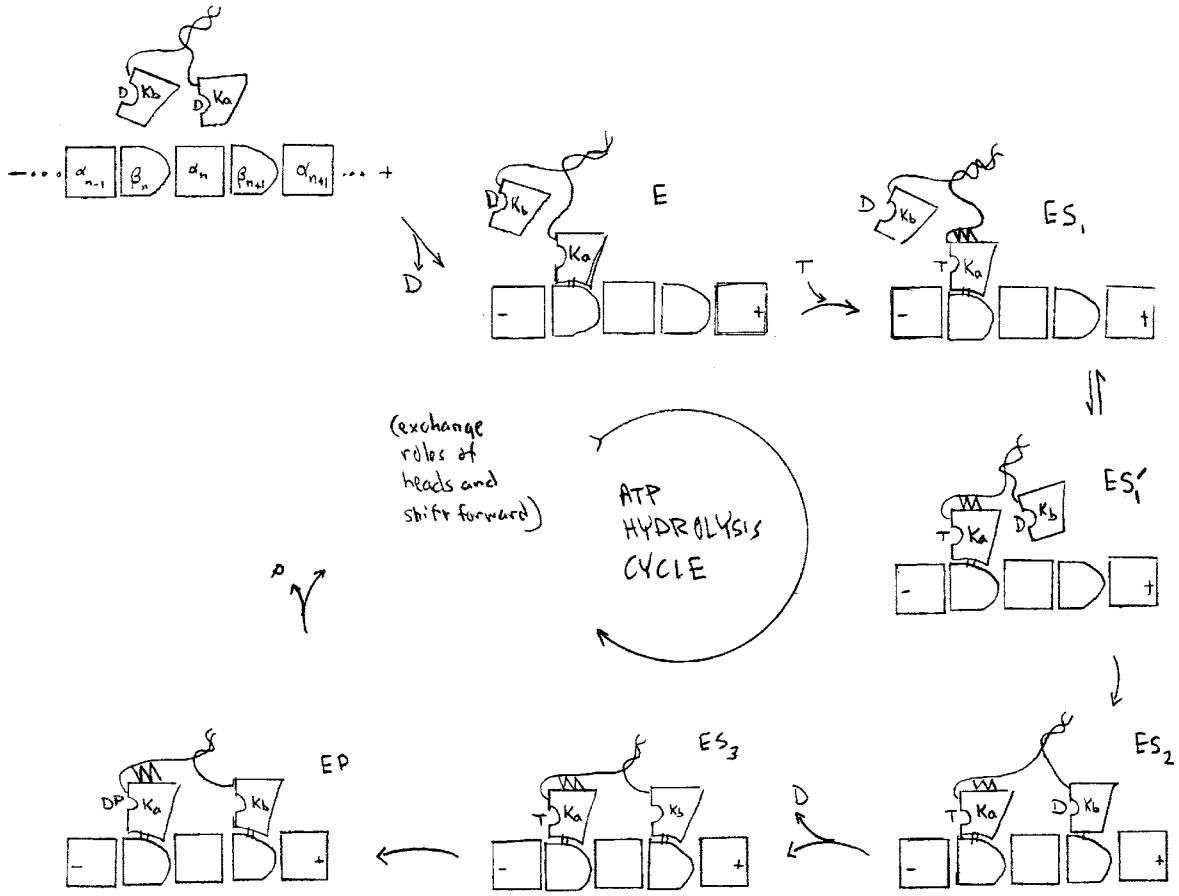


Figure 10.21: (Schematic.) One plausible model for directed motion of two-headed kinesin. Each of the steps in this cyclic reaction is described in the text starting on page 388. Several elements of this mechanism are still under debate, including the hand-over-hand character of the cycle. The eight steps form a loop, to be read clockwise from upper center. The rows of units labeled $\alpha\beta\alpha\beta\ldots$ represent a microtubule, with its "+" end at the right. Strong physical bonds are denoted by multiple lines, weak ones by single lines. The symbols K, T, D, and P denote kinesin, ATP, ADP, and inorganic phosphate, respectively. The rapid isomerization step, $\mathrm{ES}_1 \rightleftharpoons \mathrm{ES}_1'$, is assumed to be nearly in equilibrium. The states denoted $\mathrm{ES}_3$ and EP are under internal strain, as described in the text. After one complete loop the kinesin dimer has moved one step, or 8 nm, to the right, and the two kinesin heads have exchanged roles. [Similar schemes, with some variations, appear in Gilbert et al., 1998; Rice et al., 1999; Schnitzer et al., 2000; Vale & Milligan, 2000; Schief & Howard, 2001; Mogilner et al., 2001; Uemura et al., 2002.]

Later work showed that in fact two-headed kinesin is tightly coupled: It takes exactly one spatial step for each ATP molecule it consumes, even under moderate load. From the discussion at the start of this subsection, then, we may expect that two-headed kinesin would obey MM kinetics, with load-dependent parameters. Several experimental groups confirmed this prediction (Figure 10.23). Specifically, Table 10.1 shows that $v_{\max}$ decreases with increasing load, while $K_{\mathrm{M}}$ increases.

**Your Turn 10e**

The load forces tabulated in Table 10.1 reflect the force of the optical trap on the bead. But the bead experiences another retarding force, namely that of viscous friction. Shouldn't this force be included when we analyze the experiments?

Let us see what these results tell us about the details of the mechanism of force generation by

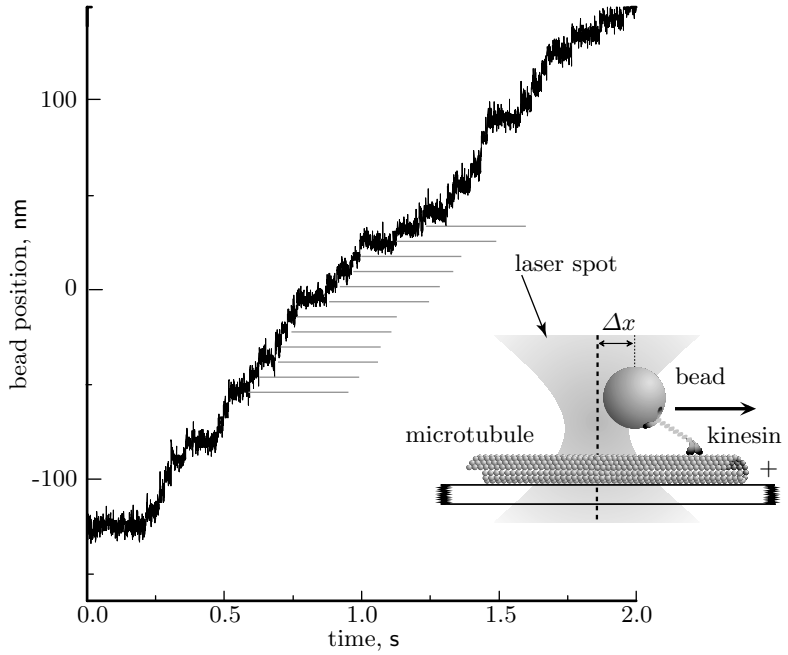


Figure 10.22: (Experimental data, with schematic.) Sample data from a kinesin motility assay. *Inset:* An optical tweezers apparatus pulls a 0.5 $\mu$m bead against the direction of kinesin stepping (not drawn to scale). A feedback circuit continuously moves the trap (gray hourglass shape) in response to the kinesin's stepping, maintaining a fixed displacement $\Delta x$ from the center of the trap and hence a fixed backward load force ("force clamping"). *Graph:* Stepping motion of the bead under a load force of 6.5 pN, with 2 mM ATP. The gray lines are separated by intervals of 7.95 nm; each corresponds to a plateau in the data. [After Visscher et al., 1999.]

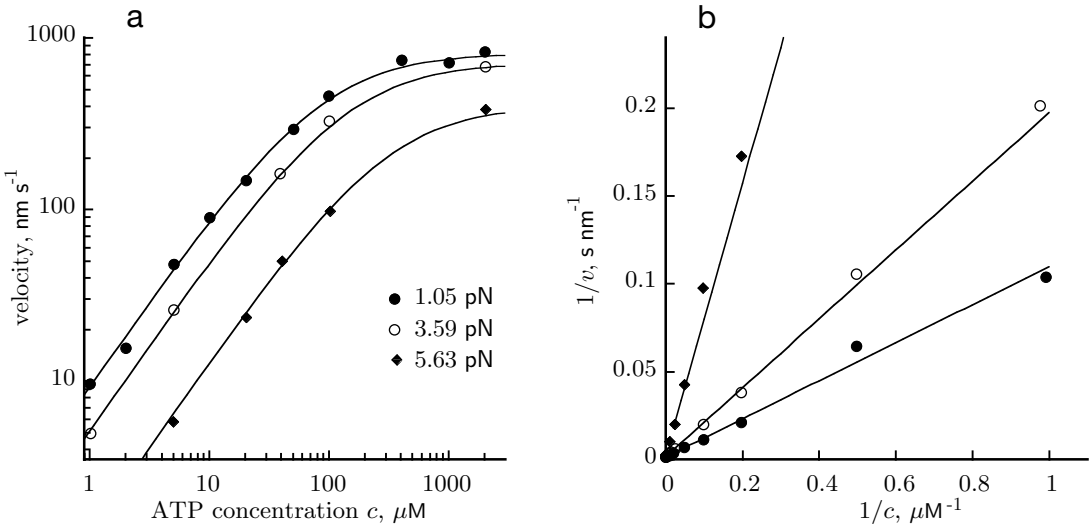


Figure 10.23: (Experimental data.) (a) Log-log plot of the speed $v$ of kinesin stepping versus ATP concentration, at various loads (see legend). For each value of load, the data were fit to the Michaelis–Menten rule, yielding the solid curves with the parameter values listed in Table 10.1. (b) Lineweaver–Burk plot of the same data. [Data from Visscher et al., 1999.]

kinesin.

One reasonable-sounding model for the stepping of kinesin might be the following: Suppose that binding of ATP is a purely chemical step, but its subsequent hydrolysis and release entail forward motion—a **power stroke**. Referring to Figure 10.17b on page 375, this proposal amounts to assuming that the load force pulls the second or third activation barrier up without affecting the first one; in the language of Equation 10.16, load reduces $k_2$ without affecting $k_1$ or $k_{-1}$. We already know how such a change will affect the kinetics: Equation 10.19 predicts that $v_{\max}$ will decrease with load (as observed), while $K_{\mathrm{M}}$ will also decrease (contrary to observation). Thus the data in Table 10.1 rule out this model.

Apparently there is another effect of load besides slowing down a combined hydrolysis/motion step. Schnitzer and coauthors proposed a model almost as simple as the unsuccessful one above to explain their data. Before describing their proposed mechanism, we must digress to summarize some prior structural and biochemical studies.

**Structural clues** The microtubule itself also has a dimeric structure, with two alternating subunit types (Figure 10.21). One of the two subunits, called "$\beta$," has a binding site for kinesin; these sites are regularly spaced at 8 nm intervals. The microtubule has a **polarity**; the subunits are all oriented in the same direction relative to each other, giving the whole structure a definite "front" and "back." We call the front the "+ end of the microtubule." Since protein binding is stereospecific (two matching binding sites must be oriented in a particular way), any bound kinesin molecule will point in a definite direction on the microtubule.

Each head of the kinesin dimer has a binding site for the microtubule, and a second binding site for a nucleotide, such as ATP. Each kinesin head also has a short (15 amino-acid) chain called the **neck linker**. The neck linkers in turn attach to longer chains. The two heads of the kinesin dimer are joined only via these chains, which intertwine, as shown schematically in Figure 10.21 on page 384. As sketched in the figure, the distance between the heads is normally too short for the dimer to act as a bridge between two binding sites on the microtubule.

One further structural observation holds another clue to the puzzle just mentioned. Chapter 9 metioned that the neck linker adopts strikingly different conformations depending on the occupancy of the nucleotide-binding site (see Figure 9.11 on page 332). When the site is empty, or occupied by ADP, the neck linker flops between at least two different conformations. When the site contains ATP, however, the neck linker binds tightly to the core of the kinesin head in a single, well-defined orientation, pointing toward the "+" end of the microtubule. This allosteric change is critical for motility: A modified kinesin, with its neck linker permanently attached to the head, was found to be unable to walk.

Table 10.1: Michaelis–Menten parameters for conventional kinesin stepping at fixed load force. [Data from Schnitzer et al., 2000.]

| load force (pN) | $v_{\max}$ (nm s$^{-1}$) | $K_{\mathrm{M}}$ ($\mu$M) |
|---|---|---|
| 1.05 | $813 \pm 28$ | $88 \pm 7$ |
| 3.6 | $715 \pm 19$ | $140 \pm 6$ |
| 5.6 | $404 \pm 32$ | $312 \pm 49$ |

**Biochemical clues** We make the abbreviations K, M, T, D for a single kinesin head, the microtubule, ATP, and ADP respectively; DP represents the hydrolyzed combination ADP·$P_i$. In the absence of microtubules, kinesin binds ATP, hydrolyzes it, releases $P_i$, then stops—the rate of release for bound ADP is negligibly small. Thus kinesin alone has very little ATPase activity.

The situation changes if one removes the excess ATP and flows the solution of K·D (kinesin bound to ADP) onto microtubules. D. Hackney found in 1994 that in this case, single-headed (monomeric) kinesin rapidly releases all its bound ADP upon binding to the microtubules. Remarkably, Hackney also found that two-headed kinesin rapidly releases *half* of its bound ADP, retaining the rest. These and other results suggested that

- Kinesin binds ADP strongly, and
- Kinesin without bound nucleotide binds microtubules strongly, but
- The complex M·K·D is only weakly bound.

In other words, an allosteric interaction within one head of kinesin prevents it from binding strongly to both a microtubule and an ADP molecule at the same time. Thus the weakly bound complex M·K·D can readily dissociate. Hackney proposed that the reason why only half of the ADP was released by kinesin dimers upon binding to microtubules was that only one head could reach a microtubule binding site at any time (top center panel of Figure 10.21).

It's hard to assess the ability of the complex K·T to bind microtubules, since the ATP molecule is short-lived (kinesin splits it). To overcome this difficulty, experimenters used an ATP analog molecule. This molecule, called AMP-PNP, has a shape and binding properties similar to those of ATP, but it does not split. Its complex with kinesin turned out to bind strongly to microtubules.

We can now state the key experimental observation. Suppose we add two-headed $(K{\cdot}D)_2$ to microtubules, releasing half of the bound ADP as above. *Adding ATP then causes the rapid release of the other half of the bound ADP!* Indeed, even the analog molecule AMP-PNP works: Binding, not hydrolysis, of nucleotide is sufficient. Somehow the unoccupied kinesin head, strongly bound to the microtubule, communicates the fact that it has bound an ATP to its partner head, stimulating the latter to release its ADP. This collaboration is remarkable, in the light of the rather loose connection between the two heads; it is not easy to imagine an allosteric interaction across such a floppy system.

In the rest of this section we need to interpret these surprising phenomena, and see how they can lead to a provisional model for the mechanochemical cycle of two-headed kinesin.

**Provisional model: Assumptions** Some of the assumptions below remain controversial, so some of the details may change in the future. Still, we'll see that the model makes definite, and tested, predictions about the load-dependence of kinesin's stepping kinetics.

We make the following assumptions, based in the clues listed earlier:

A1. We first assume that in the complexes M·K·T and M·K·DP, the kinesin binds (or "docks") its neck linker tightly, in a position that throws the attached chain forward, toward the "+" end of the microtubule. The other kinesin head in the dimer will then also get thrown forward. The states M·K and M·K·D, in contrast, have the neck linker in a flexible state.

A2. When the neck linker is docked, the detached kinesin head will spend most of its time in front of the bound head. Nevertheless, the detached head will spend *some* of its time to the rear of its partner.

A3. We assume that kinesin with no nucleotide binds strongly to the microtubule, as does K·T.

The weakly bound state M·K·D readily dissociates, either to M+K·D or to M·K+D.

Assumption A3 says that the free energy gain from ATP hydrolysis and phosphate release is partly spent on a conformational change that pulls the M·K·T complex out of a deep potential-energy well to a shallower one. Similarly, A1 says that some of this free energy goes to relax the head's grip on its neck linker. One more geometric assumption will be explained below.

**Provisional model: Mechanism** The proposed mechanism is summarized graphically in Figure 10.21 on page 384. This cycle is not meant to be taken literally; it just shows some of the distinct steps in the enzymatic pathway. Initially (top-left panel of the figure), a kinesin dimer approaches the microtubule from solution and binds one head, releasing one of its ADPs. We name the subsequent states in the ATP hydrolysis cycle by abbreviations describing the state of the head labeled "$K_a$."

E: The top-middle panel shows the dimer with $K_a$ bound to the microtubule. The other, free head $K_b$ cannot reach any binding site, because its tether is too short; the sites are separated by a fixed distance along the rigid microtubule.

$ES_1$,$ES_1'$: $K_a$ binds an ATP molecule from solution. Its neck linker then docks onto its head, biasing the other head's random motion in the forward direction (assumption A2). Schnitzer and coauthors assumed that $K_b$'s interactions with the microtubule effectively give it a weak energy landscape, so that it hops between two distinct states $ES_1$ and $ES_1'$.

$ES_2$: The chains joining the two heads will have entropic elasticity, as discussed in Chapter 9. Being thrown forward by $K_a$'s neck linker greatly increases the probability that $K_b$'s tether will momentarily stretch far enough to reach the next binding site. It may bind weakly, then detach, many times.

$ES_3$: Eventually, instead of detaching, $K_b$ releases its ADP and binds strongly to the microtubule. Its stretched tether now places the dimer under sustained strain. Both heads are now tightly bound to the microtubule, however, so the strain does not pull either one off.

EP: Meanwhile, $K_a$ splits its ATP and releases the resulting phosphate. This weakens its binding to the microtubule (assumption A3). The strain induced by the binding of $K_b$ then biases $K_a$ to unbind from the microtubule (rather than releasing its ADP).

E: The cycle is now ready to repeat, with the roles of $K_a$ and $K_b$ reversed. The kinesin dimer has made one 8 nm step and hydrolyzed one ATP.

The assumptions made above ensure that *free* kinesin (not bound to any microtubule) does not waste any of the available ATP, as observed experimentally. According to assumption A3, free kinesin will bind and hydrolyze ATP at each of its two heads, then stop, because the resulting ADPs are both tightly bound in the absence of a microtubule.

Our model is certainly more complicated than the S-ratchet device imagined in Section 10.2.2! But we can see how our assumptions implement the necessary conditions for a molecular motor found there (Idea 10.9a,b on page 369):

- The forward flip induced by neck linker binding (assumption A1), together with the polarity of the microtubule, creates the needed spatial asymmetry.
- The tight linkage to the hydrolysis of ATP creates the needed out-of-equilibrium condition, since the cell maintains the reaction quotient $c_{\mathrm{ATP}}/(c_{\mathrm{ADP}}c_{\mathrm{P_i}})$ at a level much higher than its equilibrium value.

Let us see how to make these ideas quantitative.

**Kinetic predictions** We simplify the problem by lumping all the states other than $ES_1$ and $ES_1'$ into a single state called E, just as Equation 10.16 on page 380 lumped EP with E. The model sketched in Figure 10.21 then amounts to splitting the bound state ES of the Michaelis–Menten model into two substates, $ES_1$ and $ES_1'$. To extract predictions from this model, Schnitzer and coauthors proposed that *the step* $ES_1 \rightleftharpoons ES_1'$ *is nearly in equilibrium.* That is, they assumed that the activation barrier to this transition is small enough, and hence the step is rapid enough compared to the others, that the relative populations of the two states stay close to their equilibrium values.[11] We can consider these two states together, thinking of them jointly as a **composite state**. In the language of Equation 10.16, the fraction of time spent in $ES_1$ effectively lowers the rate $k_2$ of leaving the composite state in the forward direction. Similarly, the fraction of time spent in $ES_1'$ effectively lowers the rate $k_{-1}$ of leaving the composite state in the backward direction.

We wish to understand the effect of an applied load force, that is, an external force directed away from the "+" end of the microtubule. To do this, note that the step $ES_1 \rightharpoonup ES_1'$, besides throwing head $K_b$ forward, also moves the common connecting chains to a new average position, shifted forward by some distance $\ell$. All we know about $\ell$ is that it is greater than zero, but less than a full step of 8 nm. Since a spatial step does work against the external load, the applied load force will affect the composite state: It shifts the equilibrium away from $ES_1'$ and toward $ES_1$. Schnitzer and coauthors neglected other possible load dependences, focusing only on this one effect.

We now apply the arguments of the previous two paragraphs to the definitions of the MM parameters (Equation 10.19 on page 380), finding that load reduces $v_{\max}$, as observed, and moreover may increase $K_M$ by effectively increasing $k_{-1}$ by more than it reduces $k_2$. Thus we have the possibility of explaining the data in Table 10.1 with the proposed mechanism.

To see if the mechanism works we must see if it can model the actual data. That is, we must see if we can choose the free energy change $\Delta G$ of the isomerization $ES_1 \rightleftharpoons ES_1'$, as well as the substep length $\ell$, in a way that explains the numbers in Table 10.1. Some mathematical details are given in Section 10.4.3′ on page 401. A reasonably good fit can indeed be found (Figure 10.24). More important than the literal fit shown is the observation that the simplest power-stroke model does not fit the data, but an almost equally simple model, based on structural and biochemical clues, reproduces the qualitative facts of Michaelis–Menten kinetics, with $K_M$ rising and $v_{\max}$ falling as the load is increased.

The fit value of the equilibrium constant for the isomerization reaction is reasonable: It corresponds to a $\Delta G^0$ of about $-5k_BT_r$. The fit value of $\ell$ is about 4 nm, which is also reasonable: It's half the full step length. The existence of these substeps is a key prediction of the model.

T2 *Section 10.4.3′ on page 401 completes the analysis, obtaining the relation between speed, load, and ATP availability in this model.*

### 10.4.4 Molecular motors can move even without tight coupling or a power stroke

Section 10.4.3 argued that deep within the details of kinesin's mechanochemical cycle, there lies a simple mechanism: Two-headed kinesin slides down a valley in its free energy landscape. Even while admitting that the basic idea is simple, though, we can still marvel at the elaborate mechanism

[11] Some authors refer to this assumption as "rapid isomerization."

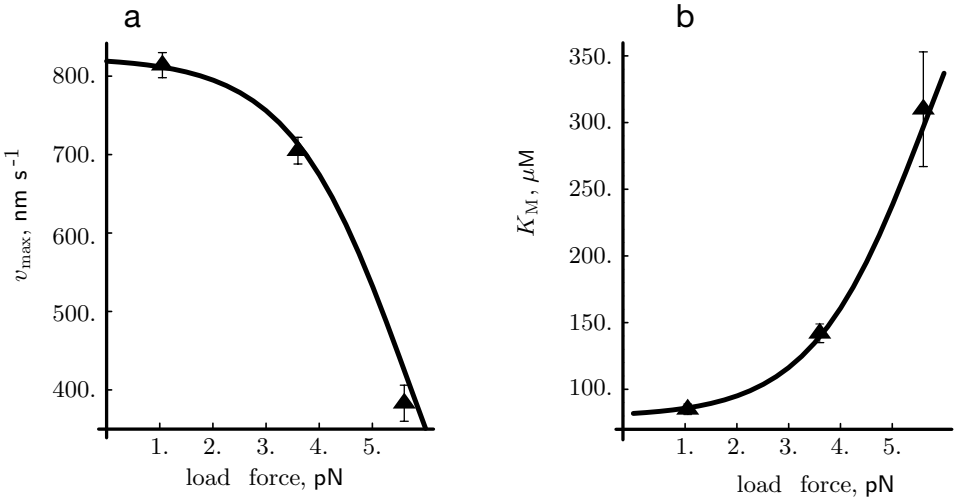


Figure 10.24: (Experimental data with fit.) Dependence of kinesin's MM parameters on applied load. Points denote the data derived from Figure 10.23 (see Table 10.1). The curves show Equations 10.31 and 10.30 respectively, with the fit parameter values given in Section 10.4.3′ on page 401.

which evolution has had to create in order to implement it. For example, we saw that in order to have a high duty ratio, kinesin has been cunningly designed to coordinate the action of its two heads. How could such a complex motor have evolved from something simpler?

We could put the matter differently by asking, "Isn't there some simpler force-generating mechanism, perhaps not as efficient or powerful as two-headed kinesin, which could have been its evolutionary precursor?" In fact, even a single-headed (monomeric) form of kinesin, called KIF1A, has been found to have single-molecule motor activity. Y. Okada and N. Hirokawa studied a modified form of this kinesin, which they called C351. They labeled their motor molecules with fluorescent dye, then watched as successive motors encountered a microtubule, bound to it, and began to walk (see Figure 2.27 on page 55).

Quantitative measurements of the resulting motion led Okada and Hirokawa to conclude that C351 operates as a **diffusing ratchet** (or "D-ratchet"). In this class of models the operating cycle includes a step involving unconstrained diffusive motion, unlike the G- and S-ratchets. Also, in place of the unspecified agent resetting the bolts in the S-ratchet (see Section 10.2.3), the D-ratchet couples its spatial motion to a chemical reaction.

The free energy landscape of a single-headed motor cannot look like our sketch, Figure 10.9 on page 362. To make progress, the motor must periodically detach from its track; once detached, it's free to move along the track. In the gear metaphor (Figure 10.6c on page 359), this means that the gears disengage on every step, allowing free slipping; in the landscape language, there are certain points in the chemical cycle (certain values of $\alpha$) at which the landscape is *flat* in the $\beta$ direction. Thus there are no well-defined diagonal valleys in the landscape. How can such a device make net progress?

The key observation is that while the grooved landscape of Figure 10.9 was convenient for us (it made the landscape effectively one-dimensional), still such a structure isn't really necessary for net motion. Idea 10.9a,b on page 369 gave the requirements for net motion as simply *a spatial asymmetry in the track, and some out-of-equilibrium process coupled to spatial location.* In principle,

we should expect that solving the Smoluchowski equation on *any* two-dimensional free energy landscape will reveal net motion, as long as the landscape is tilted in the chemical ($\alpha$) direction and asymmetric in the spatial ($\beta$) direction.

As mentioned earlier, however, it's not easy to solve the Smoluchowski equation (Equation 10.4 on page 367) in two dimensions, nor do we even know a realistic free energy landscape for any real motor. To show the essence of the D-ratchet mechanism, then, we will as usual construct a simplified mathematical model. Our model motor will contain a catalytic site, which hydrolyzes ATP, and another site, which binds to the microtubule. We will assume that an allosteric interaction couples the ATPase cycle to the microtubule binding, in a particular way:

1. The chemical cycle is autonomous—it's not significantly affected by the interaction with the microtubule. The motor snaps back and forth between two states, which we will call "s" (or "strong-binding") and "w" (or "weak-binding"). After entering the "s" state, it waits an average time $t_s$ before snapping over to "w"; after entering the "w" state it waits some other average time, $t_w$, before snapping back to "s." (One of these states could be the one with the nucleotide-binding site empty, and the other one E·ATP, as drawn in Figure 10.25.) The assumption is that $t_s$ and $t_w$ are both independent of the motor's position $x$ along the microtubule.
2. However, the binding energy of the motor to the microtubule does depend on the state of the chemical cycle. Specifically, we will assume that in the "s" state, the motor prefers to sit at specific binding sites on the microtubule, separated by a distance of 8 nm. In the "w" state, the motor will be assumed to have no positional preference at all—it diffuses freely along the microtubule.
3. In the strongly binding state, the motor feels an asymmetric (that is, lopsided) potential energy $U(x)$ as a function of its position $x$. This potential is sketched as the sawtooth curve in Figure 10.25a; asymmetry means that this curve is not the same if we flip it end-for-end. Indeed, we do expect the microtubule, a polar structure, to give rise to such an asymmetric potential.

In the D-ratchet model the free energy of ATP hydrolysis can be thought of as entering the motion solely by an assumed allosteric conformational change, which alternately glues the motor onto the nearest binding site, then pries it off. To simplify the math, we will assume that the motor spends enough time in the "s" state to find a binding site, then binds and stays there until the next switch to the "w" state.

Let's see how the three assumptions listed above yield directed motion, following the left panels of Figure 10.25. As in Section 10.2.3, imagine a collection of *many* motor-microtubule systems, all starting at one position, $x = 0$ (panels (b1) and (b2)). At later times we then seek the probability distribution $P(x)$ to find the motor at various positions $x$. At time zero the motor snaps from "s" to "w." The motor then diffuses freely along the track (panel (c1)), so its probability distribution spreads out into a Gaussian centered on $x_0$ (panel (c2)). After an average wait of $t_w$, the motor snaps back to its "s" state. Now it suddenly finds itself strongly attracted to the periodically spaced binding sites. Accordingly, it drifts rapidly down the gradient of $U(x)$ to the first such minimum, leading to the probability distribution symbolized by Figure 10.25(d2). The cycle then repeats.

The key observation is now that the average position of the motor after one cycle is now shifted relative to where it was originally. Some of this shift may arise from conformational changes, "power stroke" shifts analogous to those in myosin or two-headed kinesin. But the surprise is that

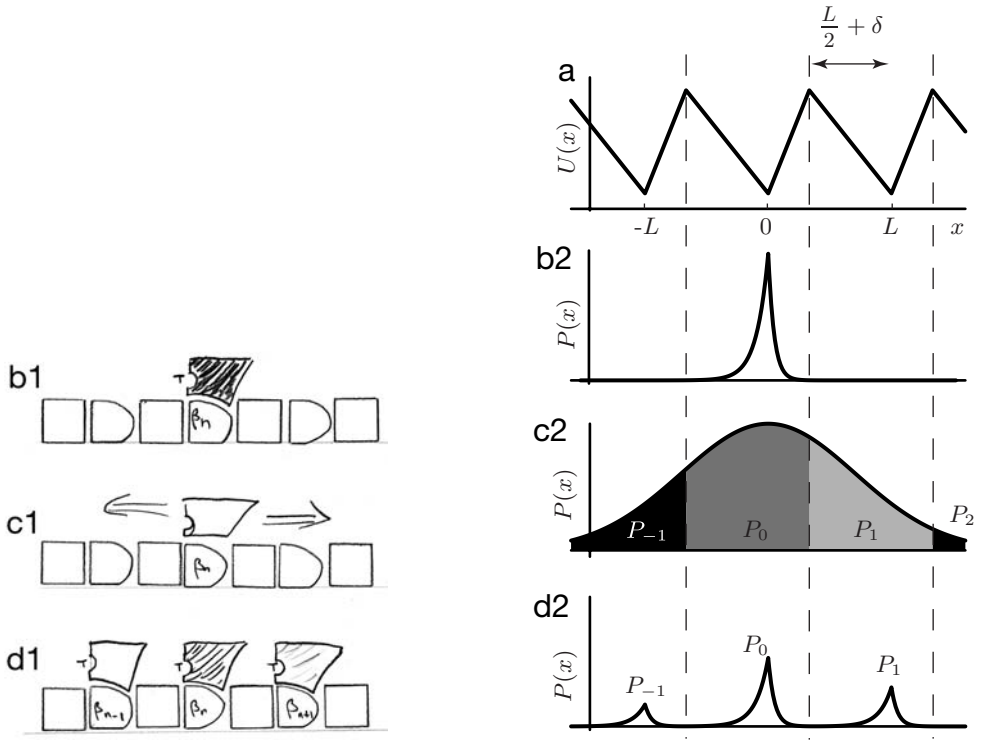


Figure 10.25: (Schematic; sketch graphs.) Diffusing ratchet (or "D-ratchet") model for single-headed kinesin motility. *Left panels:* Bound ATP is denoted by "T"; ADP and $P_i$ molecules are not shown. As in Figure 10.21, the beta subunits of the microtubule are denoted $\beta_n$. (b1) Initially the kinesin monomer is strongly bound to site $n$ on the microtubule. (c1) In the weakly bound state the kinesin wanders freely along the microtubule. (d1) When the kinesin reenters the strongly bound state, it is most likely to rebind to its original site, somewhat likely to rebind to the next site, and least likely to bind to the previous site. Relative probabilities are represented by shading. *Right panels:* (a) A periodic but asymmetric potential for the strongly bound ("s") state, as a function of position $x$ along the microtubule track. The minimum of the potential is not midway between the maxima, but rather is shifted by a distance $\delta$. The potential repeats every distance $L$ ($L = 8\,\mathrm{nm}$ for a microtubule). (b2) Quasi-equilibrium probability distribution for a motor in its "s" state, trapped in the neighborhood of the minimum at $x = 0$. The motor now suddenly switches to its "w" (or weakly binding) state. (c2) (Change of vertical scale.) The probability distribution just before the motor switches out of its "w" state. The dark gray region represents all the motors in an initial ensemble that are about to fall back into the microtubule binding site at $x = 0$; the area under this part of the curve is $P_0$. The light gray region represents those motors about to fall into the site at $x = L$; the corresponding area is $P_1$. The black regions to the left and right have areas $P_{-1}$ and $P_2$, respectively. (d2) (Change of vertical scale.) The probability distribution just before the motor switches back to the "w" state. The areas $P_k$ from (c2) have each collapsed to sharp spikes. Since $P_1 > P_{-1}$, the mean position has shifted slightly to the right.

there will be a net shift even without any power stroke! To see this, examine Figure 10.25 and its caption. The dark gray part of the curve in panel (c2) of the figure represents all the motors in the original collection that are about to rebind to the microtubule at their original position, $x = 0$. Thus the probability of taking *no* step is the area $P_0$ under this part of the curve. The two flanking parts of the curve, black and light gray, represent respectively those motors about to rebind to the microtubule at positions shifted by $-L$ or $+L$, respectively. But the areas under these parts of the curve are not equal: $P_1 \neq P_{-1}$. The motor is more likely to diffuse over to the basin of attraction at $x = +L$ than to the one at $x = -L$, simply because the latter's boundary is farther away from the starting position.

Thus the diffusing ratchet model predicts that a one-headed molecular motor can make net

progress. Indeed, we found that *it makes net progress even if no conformational change in the motor drives it in the x direction.* The model also makes some predictions about experiments. For one thing, we see that the diffusing ratchet can make backward steps;[12] $P_{-1}$ is not zero, and can indeed be large if the motor diffuses a long way between chemical cycles. In fact, each cycle gives an independent displacement, with the same probability distribution $\{P_k\}$ for every cycle. Section 4.1.3 on page 105 analyzed the mathematics of such a random walk. The conclusion of that analysis, translated into the present situation, was that

> *The diffusing ratchet makes net progress $uL$ per step, where $u = \langle k \rangle$. The variance (mean-square spread) of the total displacement increases linearly with the number of cycles, increasing by $L^2 \times$ variance$(k)$ per cycle.* (10.23)

In our model, the steps come every $\Delta t = t_s + t_w$ on average, so we predict a constant mean velocity $v = uL/\Delta t$ and a constant rate of increase in the variance of $x$ given by

$$\langle (x(t) - vt)^2 \rangle = t \times \left( \frac{L^2}{\Delta t} \times \text{variance}(k) \right). \tag{10.24}$$

Okada and Hirokawa tested these predictions with their single-headed kinesin construct, C351. Although the optical resolution of the measurements, $0.2\,\mu\text{m}$, was too large to resolve individual steps, still Figure 10.26 shows that C351 often made net backward progress (panel (a)), unlike conventional two-headed kinesin (panel (b)). The distribution of positions at a time $t$ after the initial binding, $P(x,t)$, also showed features characteristic of the diffusing ratchet model. As predicted by Equation 10.24, the mean position moved steadily to larger values of $x$, while the variance steadily increased. In contrast, two-headed kinesin showed uniform motion with very little increase in variance (panel (b)).

To make these qualitative observations sharp, Figure 10.26c plots the observed mean-squared displacement, $\langle x(t)^2 \rangle$. According to Equation 10.24, we expect this quantity to be a quadratic function of time, namely $(vt)^2 + t\frac{L^2}{\Delta t}$variance$(k)$. The figure shows that the data fit such a function well. Okada and Hirokawa concluded that although monomeric kinesin cannot be tightly coupled, it nevertheless makes net progress in the way predicted by the diffusing ratchet model.

Subtracting away the $(vt)^2$ term to focus attention on the diffusive part reveals a big difference between one- and two-headed kinesin. Figure 10.26d shows that both forms obey Equation 10.24, but with a far greater diffusion constant of proportionality for C351, reflecting the loosely coupled character of single-headed kinesin.

To end this section, let us return to the question that motivated it: How could molecular motors have evolved from something simpler? We have seen how the bare minimal requirements for a motor are simple, indeed:

- It must cyclically process some substrate like ATP, in order to generate out-of-equilibrium fluctuations.
- These fluctuations must in turn couple allosterically to the binding affinity for another protein.
- The latter protein must be an asymmetric polymer track.

It's not so difficult to imagine how an ATPase enzyme could gain a specific protein-binding site by genetic reshuffling; the required allosteric coupling would arise naturally from the general fact that all parts of a protein are tied together. Indeed a related class of enzymes is already known in

[12] Compare Problem 4.1.

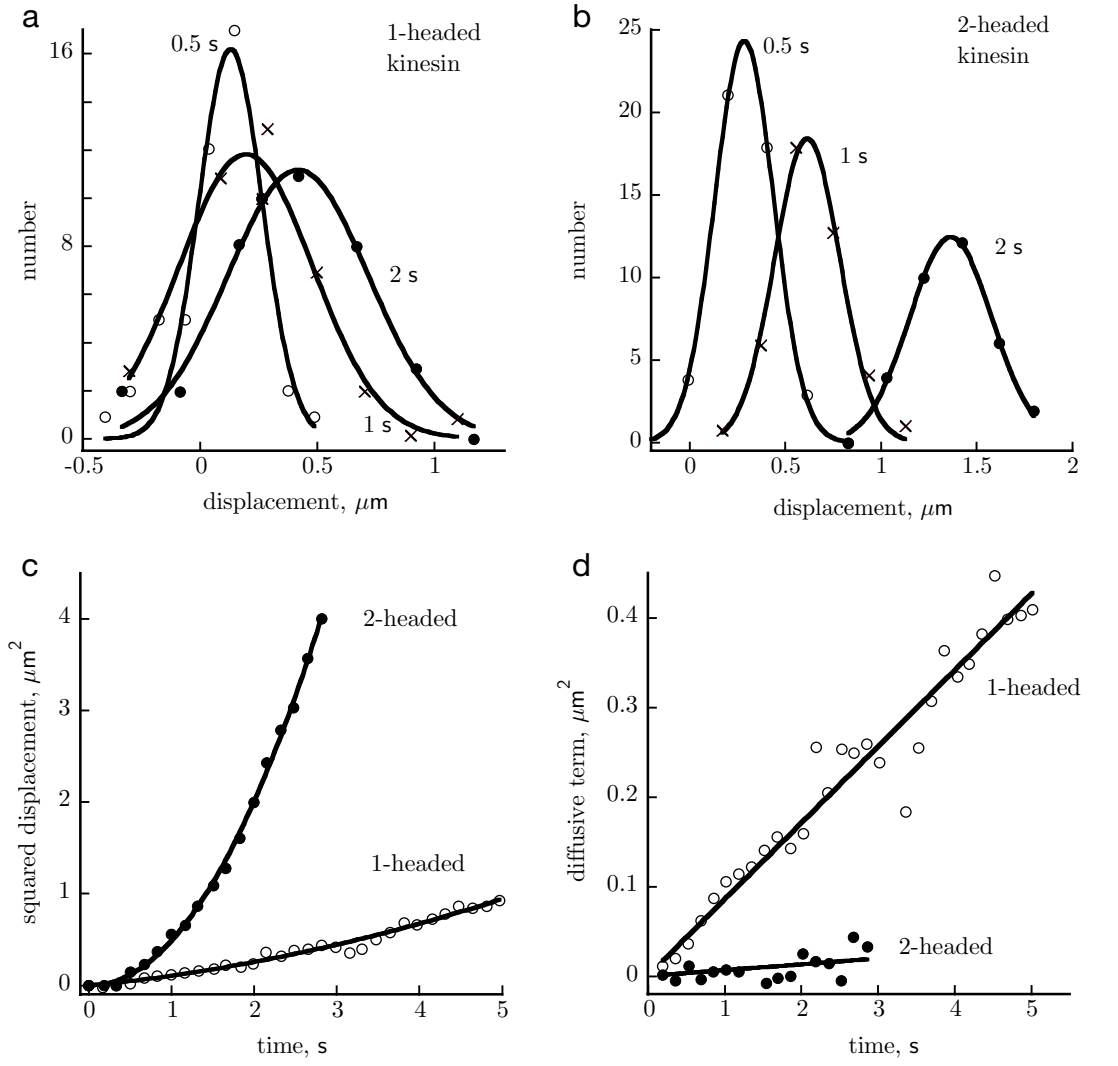


Figure 10.26: (Experimental data.) Analysis of the movement of single kinesin molecules. (a) Data for C351, a single-headed form of kinesin. The graphs give the observed distributions of displacement $x$ from the original binding site, at three different times. The solid curves show the best Gaussian fit to each dataset. Notice that even at 2 s a significant fraction of all the kinesins has made net *backward* progress. (b) The same data as (a), but for conventional two-headed kinesin. None of the observed molecules made net backward progress. (c) Mean-square displacement, $\langle x(t)^2 \rangle$, as a function of time for single-headed (open circles) and two-headed (solid dots) kinesin. The solid curves show the best fits to the predicted random-walk law (see text). (d) The same data and fits as (c), after subtracting the $(vt)^2$ term (see text). [Data from Okada & Hirokawa, 1999.]

eukaryotic cells, the "GTP-binding proteins" (or **G-proteins**); they play a number of intracellular signalling roles, including a key step in the detection of light in your retina. It seems reasonable to suppose that the first, primitive motors were G-proteins whose binding targets were polymerizing proteins, like tubulin. Interestingly, G-proteins have indeed turned out to have close structural links to both kinesin and myosin, perhaps reflecting a common evolutionary ancestry.

T2 *Section 10.4.4′ on page 402 gives some quantitative analysis of the model and compares it to the experimental data.*

Table 10.2: Examples of proteins that are believed to act as molecular motors. [From Vale, 1999.]

| Motor | Force-generating partner | Energy source | Motion | Role and features |
|---|---|---|---|---|
| **Cytoskeleletal motors** | | | | |
| Kinesin | Microtubule | ATP | Linear | Mitosis/organelle transport, microtubule dynamics |
| Myosin | Actin | ATP | Linear | Muscle contraction/organelle transport/cytokinesis |
| Dynein | Microtubule | ATP | Linear | Ciliary beating/organelle transport/mitosis<br>Motor has four ATP-binding sites |
| **Polymers** | | | | |
| Actin | None | ATP | Extend/shrink | Cell motility/cortical organization |
| Microtubule | None | GTP | Extend/shrink | Mitosis/cytoplasmic organization |
| Dynamin | Membranes | GTP | Pinching | Endocytosis/vesicle budding |
| Spasmin/centrin | None? | $Ca^{2+}$ | Contraction | Contraction |
| **G proteins** | | | | |
| EfG | Ribosome | GTP | Lever | Movement of peptidyl-tRNA, mRNA in the ribosome |
| **Rotary motors** | | | | |
| $F_1$ ATPase | $F_o$ complex | ATP | Rotary | ATP synthesis/hydrolysis, reversible/100% efficient |
| Bacterial flagellar | Many proteins | $H^+/Na^+$ | Rotary | Bacterial propulsion, rapidly reversible motor |
| **Rings** | | | | |
| AAA proteins | Various partners | ATP | Twisting? | Disruption of protein–protein interactions |
| GroEl | GroES, unfolded protein | ATP | Prying | Protein folding |
| **Nucleic acid motors** | | | | |
| Polymerase | DNA/RNA | ATP | Linear | Template replication |
| Helicases | DNA/RNA | ATP | Linear | Unwinding activity |
| SMC proteins | DNA, condensins | ATP | Condensation | Chromosome formation |

## 10.5 Vista: Other molecular motors

New molecular machines are being discovered at a dizzying pace. Table 10.2 lists some of the known examples from a recent review. Still other motors pack viral DNA into the virus head. Yet another class of machines transport ions across membranes against their electrochemical gradient; these "pumps" will play a key role in Chapter 11.

## The big picture

Returning to the Focus Question, this chapter has uncovered two simple requirements for a molecular device to transduce chemical energy into useful mechanical work: The motor and track must be asymmetrical, in order to select a direction of motion, and they must couple to a source of excess free energy, for example a chemical reaction that is far from equilibrium. The following chapter will introduce two other classes of molecular machines, ion pumps and the rotary ATP synthase.

A mechanochemical motor transduces chemical free energy to mechanical work. When the relative concentrations of fuel and waste differ from equilibrium, that's a form of order, analogous to the temperature differential that ran our heat engine in Section 6.5.3. It may seem surprising that the motors in this chapter can work inside a single, well-mixed chamber; in contrast, a heat engine must sit at the *junction* between a hot reservoir and a cold one. But if there is an activation barrier to the spontaneous conversion of fuel to waste, then even a well-mixed solution has an invisible wall separating the two, like a dam on a river. It's really not in equilibrium at all. The motor is like a hydroelectric plant on that dam: It offers a low-barrier pathway to the state of lower $\mu$. Molecules will rush down that pathway, even if they are required to do some work along the way, just as water rushes to drive the turbine of the hydroelectric plant.

Cells contain a staggering variety of molecular motors. This chapter has made no attempt to capture Nature's full creative range, once again focusing on the humbler question "How could anything like that that happen at all?" Nor did we attempt even a survey of the many beautiful experimental results now available. Rather, the goal was simply to create some explicit mathematical models, anchored in simpler, known phenomena and displaying some of the behavior experimentally observed in real motors. Such conceptually simple models are the armatures upon which more detailed understanding must rest.

## Key formulas

- *Perfect ratchet:* A perfect ratchet (that is, one with an irreversible step) at zero load makes progress at the rate $v = L/t_{\text{step}} = 2D/L$ (Equation 10.2).
- *Smoluchowski:* Consider a particle undergoing Brownian motion on a potential landscape $U(x)$. In a steady (not necessarily equilibrium) state, the probability $P(x)$ of finding the particle at location $x$ is a solution to (Equation 10.4)

$$0 = \frac{\mathrm{d}}{\mathrm{d}x}\left(\frac{\mathrm{d}P}{\mathrm{d}x} + \frac{1}{k_{\mathrm{B}}T}P\frac{\mathrm{d}U}{\mathrm{d}x}\right),$$

  with appropriate boundary conditions.
- *Michaelis–Menten:* Consider the catalyzed reaction $\mathrm{E} + \mathrm{S} \underset{k_{-1}}{\overset{k_1}{\rightleftharpoons}} \mathrm{ES} \overset{k_2}{\rightharpoonup} \mathrm{E} + \mathrm{P}$. A steady, nonequilibrium state can arise when the supply of substrate S is much larger than the supply of enzyme E. The reaction velocity (rate of change of substrate concentration $c_{\mathrm{S}}$) in this case is $v = v_{\max}\frac{c_{\mathrm{S}}}{K_{\mathrm{M}}+c_{\mathrm{S}}}$ (Equation 10.20), where the saturating reaction velocity is $v_{\max} = k_2 c_{\mathrm{E}}$ and the Michaelis constant is $K_{\mathrm{M}} = (k_{-1} + k_2)/k_1$ (Equation 10.19).

## Further reading

*Semipopular:*
Enzymes: Dressler & Potter, 1991.

*Intermediate:*
Enzymes: Berg et al., 2002; Voet & Voet, 2003.
Chemical kinetics: Tinoco Jr. et al., 2001; Dill & Bromberg, 2002.
From actin/myosin up to muscle: McMahon, 1984.
Ratchets: Feynman et al., 1963a, §46.
Motors: Berg et al., 2002; Howard, 2001; Bray, 2001.
Computer modeling of muscle mechanics: Hoppensteadt & Peskin, 2002.

*Technical:*
Kramers theory: Kramers, 1940; Frauenfelder & Wolynes, 1985; Hänggi et al., 1990.
The abstract discussion of motors was largely drawn from the work of four groups around 1993. Some representative reviews by these groups include Jülicher et al., 1997; Astumian, 1997; Mogilner et al., 2002; Magnasco, 1996; see also the original papers cited therein.
Single-molecule motility assays: Howard et al., 1989; Finer et al., 1994.

Myosin, kinesin, and G-proteins: general, Vale & Milligan, 2000; role of kinesin neck linker: Rice et al., 1999; Schnitzer et al., 2000; Mogilner et al., 2001.
RNA polymerase: Wang et al., 1998.
Polymerization ratchet, translocation ratchet: Mahadevan & Matsudaira, 2000.